



# Synapse Location during Growth Depends on Glia Location

Zhiyong Shao,<sup>1</sup> Shigeki Watanabe,<sup>2</sup> Ryan Christensen,<sup>1</sup> Erik M. Jorgensen,<sup>2</sup> and Daniel A. Colón-Ramos<sup>1,\*</sup>

<sup>1</sup>Program in Cellular Neuroscience, Neurodegeneration and Repair, Department of Cell Biology, Yale University School of Medicine, P.O. Box 9812, New Haven, CT 06536-0812, USA

<sup>2</sup>Howard Hughes Medical Institute, Department of Biology, University of Utah, Salt Lake City, UT 84112-0840, USA

\*Correspondence: [daniel.colon-ramos@yale.edu](mailto:daniel.colon-ramos@yale.edu)

<http://dx.doi.org/10.1016/j.cell.2013.06.028>

## SUMMARY

Synaptic contacts are largely established during embryogenesis and are then maintained during growth. To identify molecules involved in this process, we conducted a forward genetic screen in *C. elegans* and identified *cima-1*. In *cima-1* mutants, synaptic contacts are correctly established during embryogenesis, but ectopic synapses emerge during postdevelopmental growth. *cima-1* encodes a solute carrier in the SLC17 family of transporters that includes sialin, a protein that when mutated in humans results in neurological disorders. *cima-1* does not function in neurons but rather functions in the nearby epidermal cells to correctly position glia during postlarval growth. Our findings indicate that CIMA-1 antagonizes the FGF receptor (FGFR), and does so most likely by inhibiting FGFR's role in epidermal-glia adhesion rather than signaling. Our data suggest that epidermal-glia crosstalk, in this case mediated by a transporter and the FGF receptor, is vital to preserve embryonically derived circuit architecture during postdevelopmental growth.

## INTRODUCTION

The nervous system is largely established during embryogenesis, but connectivity persists throughout the lifetime of the organism (Benard and Hobert, 2009). For example, in *C. elegans*, as in other metazoans, neural circuitry is laid out largely during embryogenesis (Sulston et al., 1983). Thereafter the worm grows 100-fold in volume, yet axonal architecture and synaptic contacts are maintained (Benard and Hobert, 2009; Knight et al., 2002). Genetic studies have identified molecules required for the maintenance of axon positions during growth and movement, including L1-CAM, F-spondin, and the FGF receptor among others (Aurelio et al., 2002; Benard and Hobert, 2009; Benard et al., 2012; Benard et al., 2006; Bülow et al., 2004; Johnson and Kramer, 2012; Pocock et al., 2008; Sasakura et al., 2005; Woo et al., 2008). This work indicates two important features regarding the maintenance of nervous system architecture during development. First, the molecules

required for maintenance of axon position are distinct from those required for circuit formation. Second, these studies underscore the importance of regulated adhesion in maintenance of axon position.

Circuit architecture also requires the maintenance of synaptic contacts. Synaptic maintenance studies have largely focused on the stability of synapses (Lin and Koleske, 2010; Shi et al., 2012; Wilcox et al., 2011). From these studies we know that neuron-glia interactions can play key roles in the maintenance of synaptic stability (Pfrieger, 2010). Less is known about how synaptic distribution is maintained during postdevelopmental growth. Synaptic distribution, which is critical for maintenance of the embryonically derived circuit architecture, requires both maintenance of correct synaptic contact and prevention of formation of inappropriate contacts.

We perform a screen in *C. elegans* and identify *cima-1*. In *cima-1* mutants, inappropriate contacts between glia and axons promote the formation of ectopic synapses. Glia inappropriately contact axons in these mutants, likely due to increased adhesion with epidermal cells during growth. CIMA-1 is a SLC17 family solute transporter that modulates epidermal-glia interaction via FGFR. We reveal a potential mechanism for the role of SLC17 transporters in maintenance of synaptic distribution. Furthermore, we suggest that *reducing* adhesion during growth is as important as *promoting* adhesion to maintain correct synaptic connectivity.

## RESULTS

### AIY Synapses Form during Embryogenesis and Are Maintained during Growth

The AIY interneurons are a pair of bilaterally symmetric neurons in the nematode nerve ring (Figure 1A). Although these neurons contact many potential synaptic partners, they display remarkable specificity for both synaptic partner and position (White et al., 1986). In adult animals, the observed pattern of synaptic outputs in AIY is reproducible across animals (Colón-Ramos et al., 2007). To determine when AIY synaptic outputs are established, we examined the AIY presynaptic pattern in *C. elegans* larval stages using GFP::RAB-3 (Nonet et al., 1997). We observed that the presynaptic pattern was already established by the time the animals hatched at larval stage 1 (L1) (Figures 1A, 1B, 1C and Colón-Ramos et al., 2007). We also observed that although the length of the neurite and synaptic zones

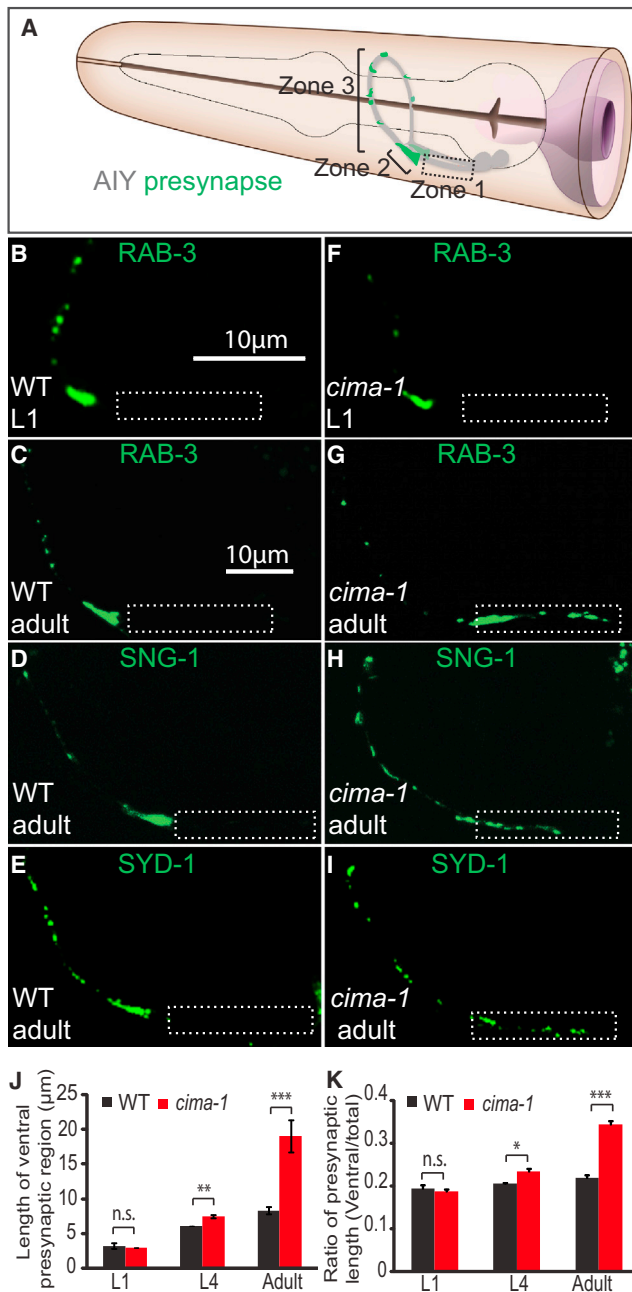


**Figure 1. *cima-1* Is Required for Maintenance of AIY Presynaptic Distribution during Growth**

(A) Schematic diagram of bilaterally symmetric AIYs (gray) in the *C. elegans* head (modified from WormAtlas with permission). Green marks presynaptic positions. There are three distinct anatomical regions along the AIY neurite: a segment proximal to AIY cell body that is devoid of synapses (zone 1, dashed box), a dense presynaptic region at the dorsal turn of the AIY neurite (zone 2), and a region with discrete presynaptic clusters at the distal part of the neurite (zone 3) (Colón-Ramos et al., 2007; White et al., 1986). Schematic illustration is a modification with permission from the Neuron pages of WormAtlas (<http://www.wormatlas.org>) by Z.F. Altun and D.H. Hall.

(B–E) The AIY presynaptic pattern in wild-type animals. Using synaptic vesicle associated GFP::RAB-3, we observe that AIY presynaptic pattern is already established in newly hatched larval L1 stage animals (B) and maintained in

increase as the animal grows, the relative distribution of presynaptic sites is maintained (Figures 1B, 1C, 1J, and 1K). Our findings indicate that the presynaptic pattern in the AIY interneuron is established during embryogenesis and is maintained as the animal grows.

### *cima-1* Inhibits Ectopic Synapses during Growth

To identify the mechanisms underlying the maintenance of synaptic distribution during growth, we performed a visual forward genetic screen and isolated *cima-1(wy84)* (for circuit maintenance). GFP::RAB-3 distribution was indistinguishable between *cima-1(wy84)* and wild-type animals at larval L1 stage (Figures 1B, 1F, 1J, and 1K). *cima-1(wy84)* adult animals, however, displayed a highly penetrant ectopic GFP::RAB-3 localization in the normally asynaptic zone 1 of AIY (Figure 1G, >90% of animals,  $n > 200$  animals). Quantification of the *cima-1(wy84)* phenotype in adult animals revealed that although the length of zone 3 remained similar between mutants and wild-type adult animals, the ventral presynaptic region (zone 2, and ectopic presynaptic structures in zone 1) was twice as long in *cima-1(wy84)* mutants (Figures 1G and 1J). The synaptic defect in *cima-1(wy84)* was confirmed using synaptic vesicle proteins SNB-1 and SNG-1, as well as active zone protein SYD-1 (Figures 1D, 1E, 1H, and 1I and data not shown). Fluorescence electron microscopy (fEM) also demonstrated the presence of ectopic presynaptic sites in *cima-1(wy84)* animals (Figure S1 available online) (Watanabe and Jorgensen, 2012; Watanabe et al., 2011). Together, our data indicate that *cima-1(wy84)* is not required for establishing presynaptic distribution but is required for maintaining it.

### Ectopic Presynaptic Sites in *cima-1* Mutants Are Not onto Postsynaptic Partner RIA

The synapses in zone 2 of wild-type animals are formed primarily onto postsynaptic partner RIA (Figure 2A and White et al., 1986). To determine whether the ectopic synapses are targeted to RIA,

adults (C). A similar pattern was observed when we visualized synaptic vesicle protein SNG-1::YFP (D) and active zone protein GFP::SYD-1 (E) in adults and L1 larva (data not shown).

(F–I) *cima-1(wy84)* mutant animals fail to maintain the AIY presynaptic pattern in adults. *cima-1(wy84)* mutant L1 animals display a wild-type presynaptic pattern as visualized with GFP::RAB-3 (F). Adult animals display an abnormal presynaptic pattern as visualized with presynaptic proteins GFP::RAB-3 (G), SNG-1::YFP (H), and GFP::SYD-1 (I). The ectopic presynaptic structure was confirmed with fluorescence electron microscopy (fEM) (Figure S1). In all images, dashed box corresponds to normally asynaptic zone 1, and scale bars are 10 μm (scale bar in [B] applies to [B] and [F]; scale bar in [C] applies to [C]–[E] and [G]–[I]).

(J and K) Quantification of the AIY presynaptic pattern. Note that the length of ventral portion of the presynaptic region (presynaptic region in zone 1 and zone 2) is similar in *cima-1(wy84)* and wild-type animals at L1 stage but becomes longer at L4 or adult stages (J). The ratio of the presynaptic length (the length of ventral presynaptic region divided by total presynaptic region as shown in [K]) is a metric that reflects the general pattern of AIY, and persists in wild-type animals during growth (black bars). Note that in *cima-1(wy84)* mutant animals this ratio becomes abnormally larger, particularly in postdevelopmental growth after the L4 stage (red bars).  $n \geq 34$  for each group. Error bars are SEM, \* $p < 0.05$ , \*\* $p < 0.01$ , \*\*\* $p < 0.001$  by t test comparison.

See also Figure S1.

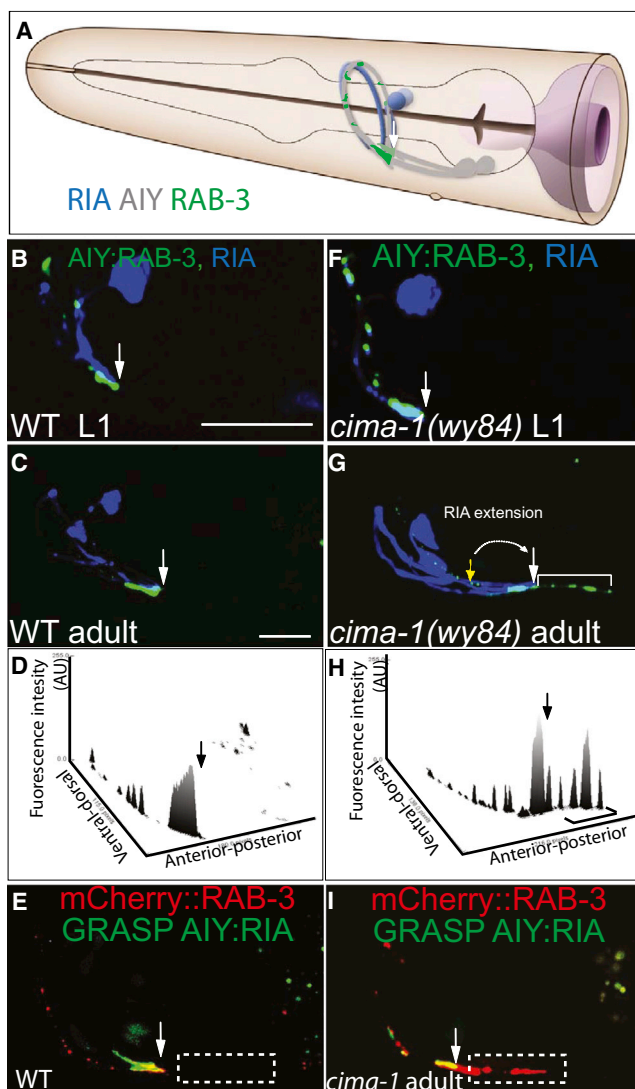


**Figure 2. *cima-1(wy84)* Mutants Have a Posteriorly Extended Zone 2 and Ectopic Presynaptic Structures in Zone 1**

(A) AIY (gray) forms synapses onto postsynaptic partner RIA (blue) in zone 2 (Colón-Ramos et al., 2007; White et al., 1986); Schematic diagram modified from WormAtlas with permission. (B and C) Simultaneous visualization of synaptic vesicles in AIY (pseudocolor green) and postsynaptic GLR-1 sites in RIA (pseudocolor blue) in a wild-type animal. Note that in both L1 (B) and adults (C), RIA contacts AIY in zone 2 and not in zone 1. The arrow indicates the transition between zone 2 and zone 1, as determined by the position where RIA contacts AIY. Schematic illustration is a modification with permission from the Neuron pages of WormAtlas (<http://www.wormatlas.org>) by Z.F. Altun and D.H. Hall.

(D) 3D profile of AIY presynaptic CFP::RAB-3 (pseudocolor green) fluorescence intensity (arbitrary units) of (C). The arrow indicates the transition between zone 2 and zone 1.

(E) Simultaneous visualization of GRASP GFP (which indicates contact between presynaptic neuron AIY and postsynaptic partner RIA) and mCherry::RAB-3 in a wild-type animal. Note that the AIY:RIA contact indicated by GFP overlaps with presynaptic mCherry::RAB-3 at zone 2 region.

(F and G) The AIY presynaptic pattern and RIA morphology are wild-type in newly hatched (L1 stage) *cima-1(wy84)* mutant animals (F). However, at the adult stage the RIA neurite is posteriorly extended (from AIY ventral turn

we simultaneously imaged RIA and the presynaptic sites in AIY. We observed that in wild-type and *cima-1(wy84)* juvenile animals, RIA projects to zone 2 correctly (Figures 2B and 2F). However, we noted two differences in the adult mutants. First, in adult *cima-1(wy84)* animals, the RIA neurite is extended posteriorly (Figure 2G). Second, we also observed ectopic presynaptic sites in zone 1 that extend beyond the area of contact between AIY and RIA (compare Figures 2C with 2G and 2D with 2H).

To further examine the relationship between AIY:RIA contact and the ectopic presynaptic sites in zone 1, we performed GFP reconstitution across synaptic partners (GRASP) (Feinberg et al., 2008). GRASP is based on two GFP fragments (“GFP 1-10” and “GFP 11”) that can reconstitute a functional GFP molecule only when they are in close proximity. A version of GRASP based on the transmembrane protein CD4 allows assessment of cell-cell contact sites (Feinberg et al., 2008). We expressed this version of GRASP in AIY (CD4::GFP 11) and RIA (CD4::GFP 1-10) to specifically visualize AIY:RIA contact and simultaneously labeled AIY presynaptic sites with mCherry::RAB-3. We observed that ectopic presynaptic sites were present beyond the AIY:RIA contact region (Figures 2E and 2I). Our studies indicate that the abnormal distribution of presynaptic structures in *cima-1(wy84)* adults results from two events: a posterior displacement of synapses between AIY and RIA in zone 2 and the emergence of ectopic presynaptic sites, which are not apposed to postsynaptic cell RIA, in zone 1.

### ***cima-1* Encodes a Membrane Transporter in the SLC17 Family**

Our SNP mapping, genetic rescue and Sanger sequencing data suggest that the *cima-1(wy84)* allele corresponds to a G to A mutation in the unnamed gene F45E4.11, and that this mutation is predicted to alter a conserved glycine at residue 388 to glutamate (Figures 3A, 3B, and 3F). A second allele of F45E4.11 (*gk902665*), with a nonsense mutation at R476, phenocopies the *cima-1(wy84)* AIY defect (Figure 3C). We also observed a similar AIY presynaptic maintenance defect when knocking down F45E4.11 by RNAi (Figures 3E). Together, our genetic data indicate that *cima-1(wy84)* is a missense, loss-of-function mutation in F45E4.11 (hereafter called *cima-1*).

*cima-1* encodes a 12 transmembrane domain protein that is homologous to the SLC17 family of solute carrier transporters

indicated by yellow arrow to the posterior site indicated by white arrow) and ectopic presynapses are seen in zone 1 (bracket) (G).

(H) 3D profile of AIY presynaptic GFP::RAB-3 fluorescence intensity (arbitrary units) of the image in (G).

(I) Simultaneous visualization of GRASP GFP and mCherry::RAB-3 in a *cima-1(wy84)* animal. Note that presynaptic mCherry::RAB-3 extends beyond the AIY:RIA contact region (indicated by GRASP GFP signal).

Ectopic presynaptic sites in AIY are bracketed. All arrows except the yellow in (G) indicate the end of zone 2 and the beginning of zone 1. The yellow arrow in (G) indicates where the end of zone 2 and the beginning of zone 1 should be. Scale bars, 10 $\mu$ m (scale bar in [B] applies to [B] and [F]; scale bar in [C] applies to [C], [G], [E] and [I]).

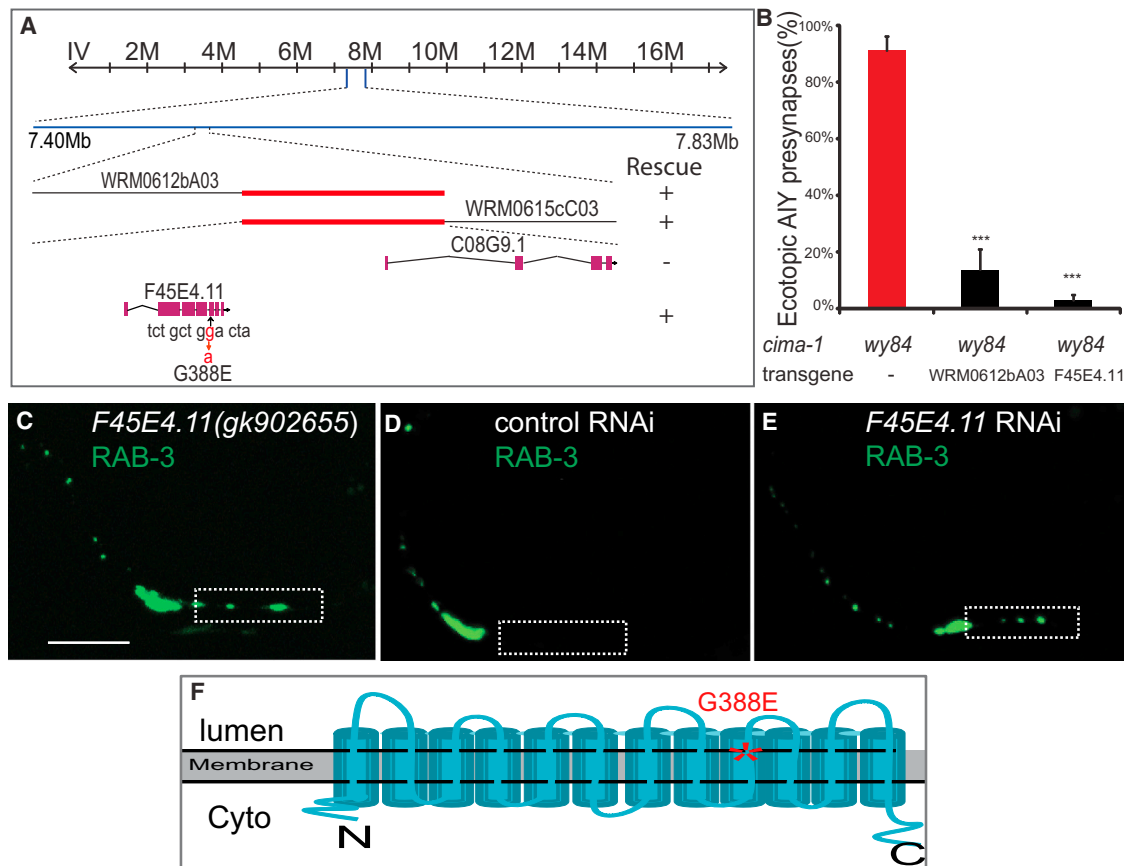


**Figure 3. *cima-1(wy84)* Is an Allele of *F45E4.11*, which Encodes a Conserved SLC17 Family Transporter**

(A) SNP mapping indicates that the genetic lesion corresponding to the *cima-1(wy84)* allele is between 7.40 Mb and 7.83 Mb on chromosome IV. Two overlapping fosmids in this region (WRM0612bA03 and WRM0615cC03) rescue the *cima-1(wy84)* AIY presynaptic defect. Those two fosmids overlap in a genomic area that includes just two genes: *F45E4.11* and *C08G9.1*. Only *F45E4.11* was able to rescue the AIY defect. Sequencing data indicate a missense mutation in the coding region that alters conserved G388 to E.

(B) Quantification of the percentage of animals displaying the AIY presynaptic patterning defect in *cima-1(wy84)* mutants transformed with fosmid WRM0612bA03 (which includes gene *F45E4.11*) or with just gene *F45E4.11*.  $n \geq 86$  for each category. Error bars are SEM, \*\*\* $p < 0.001$  by t test.

(C) A different *F45E4.11* allele, *gk902655*, contains a nonsense mutation in the coding region (R476 to opal stop codon) and phenocopies the *wy84* allele.

(D and E) Knockdown of *F45E4.11* by RNAi phenocopies the *cima-1(wy84)* presynaptic phenotype in AIY. Animals fed with bacteria transfected with control vector L4440 show normal AIY presynaptic distribution (D), whereas animals fed with bacteria expressing *F45E4.11* dsRNA phenocopy the *cima-1(wy84)* AIY presynaptic phenotype (E).

Scale bar, 10  $\mu$ m (C–E). In (C–E), zone 1 region is highlighted with a dashed box.

(F) A schematic diagram of the predicted *cima-1* topology. The mutated G388 (asterisk) in *cima-1(wy84)* is located in ninth transmembrane domain. CIMA-1 is a member of SLC17 transporter family (See also Figure S2).

and similar to sialin, a lysosomal transporter associated with neurodegenerative disease (Reimer, 2013; Sreedharan et al., 2010; Verheijen et al., 1999) (Figures 3F and S2).

#### *cima-1* Acts in Epidermal Cells

To understand the mechanism by which *cima-1* suppresses ectopic presynapses, we first examined its endogenous expression pattern. We generated a transcriptional GFP reporter and found *cima-1* expression starts during embryogenesis and persists in adult animals (Figures 4A–4D and S3A–S3H). In adults, *cima-1* is primarily expressed in epidermal cells. Expression was also observed in intestinal cells, but not in neurons (including AIY) or in glia (Figures S3E–S3H).

Consistent with the expression pattern, we observed that expression of CIMA-1 cell specifically in epidermal cells results in robust rescue of the AIY phenotype (Figure 4E and S3I). Conversely, expression of CIMA-1 cell specifically in the AIY interneurons (*ttx-3* promoter), in all neurons (*rab-3* promoter), or in neurons and intestine (*aex-3* promoter) did not rescue (Figure 4E and S3I). These data suggest that *cima-1* acts in epidermal cells to maintain the AIY presynaptic pattern.

We note that although *cima-1* is required in epidermal cells, *cima-1(wy84)* mutant animals do not exhibit obvious defects in body morphology, epidermal cell morphology, cellular fusion events, epidermal development, or general neuroarchitecture in larvae or young adults (Figure S4 and data not shown).

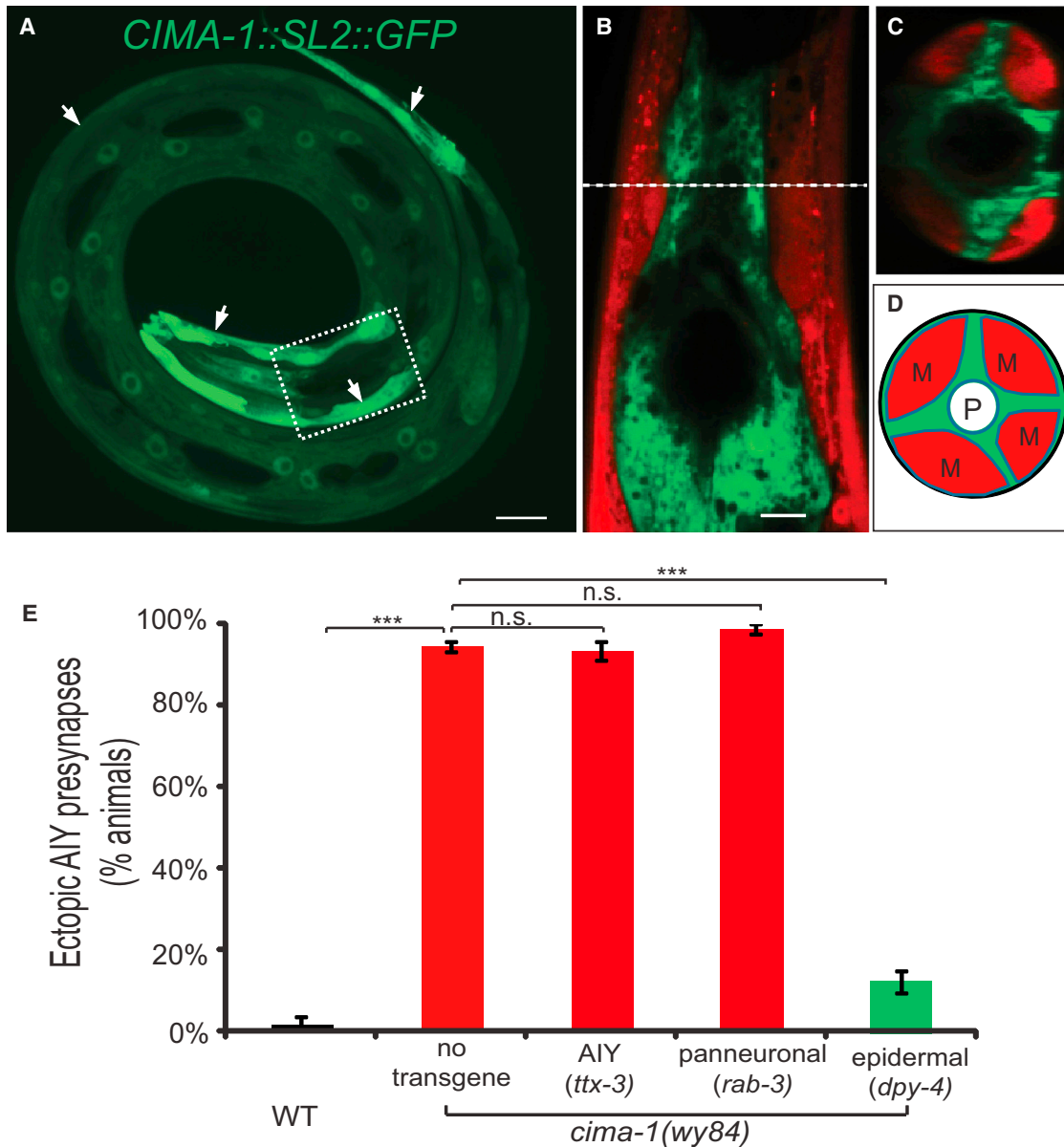


#### Figure 4. *cima-1* Is Expressed and Required in Epidermal Cells for Maintenance of the AIY Presynaptic Pattern

(A) A larval animal displaying the endogenous *cima-1* expression pattern as determined by rescuing construct *CIMA-1(genomic)::SL2::GFP*. The dashed box corresponds to the region where AIY is located (AIY not shown; this region is also similar to the region examined in [B] and [C]). Arrows point at CIMA-1-expressing epidermal cells.

(B–D) Simultaneous visualization of *cima-1(genomic)::SL2::GFP* (green) and body wall muscle reporter *Pmyo-3::mcherry* (red). Note the nonoverlapping expressing pattern of *cima-1* in epidermal cells and *Pmyo-3::mcherry* in muscles, both in the sagittal cross-section (B) and in the transverse cross-section (C). Dashed line in (B) indicates site of transverse cross-section image in (C). And (D) is the schematic drawing of (C), with muscle quadrants (“M”), epidermal cells (green) and pharynx (P) labeled.

(E) Quantification of tissue-specific rescue. Expression of *cima-1* cDNA in AIY (*ttx-3* promoter) or pan-neuronally (*rab-3* promoter) does not rescue the AIY presynaptic defect in *cima-1(wy84)* mutant animals. However, expression of *cima-1* cDNA in epidermal cells (*dpy-4* promoter) robustly rescues the AIY presynaptic defect (see also rescue with epidermal promoters *rol-6*, *dpy-7* and *col-19* in Figure S3).  $n \geq 50$  for each group. Error bars are SEM, n.s.: not significant, \*\*\* $p < 0.001$  by t test. Scale bars, 10  $\mu\text{m}$ .

See also Figures S3, S4 and S5.

Next, we wanted to determine the temporal requirement of *cima-1*. As AIY presynaptic defects are only observed in adults, we hypothesized that expression of *cima-1* after larval develop-

ment would be sufficient to rescue the AIY presynaptic defect. To test this, we expressed *cima-1* using a *col-19* promoter that expresses just in epidermal cells and after larval development

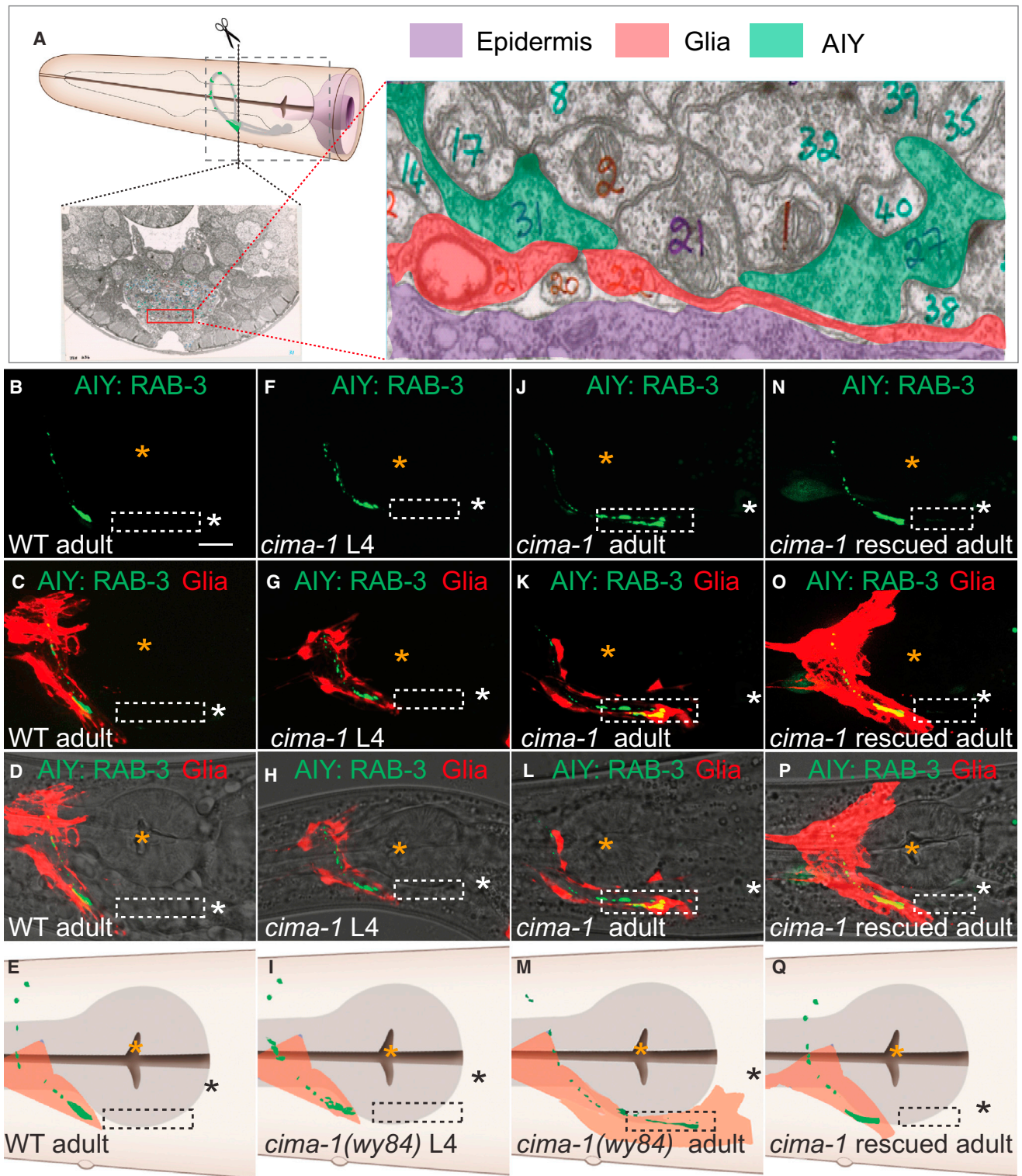


**Figure 5. *cima-1* Is Required for Maintenance of VCSC Glial Morphology during Growth**

(A) Relative position of epidermal cells, VCSC glia and AIY in *C. elegans*. A cross section of EM image of a wild-type animal in the zone 2 region of AIY (from <http://www.WormAtlas.org> and <http://www.WormImage.org>) (White et al., 1986). VCSC glia (pseudocolored red in the micrograph) lie between the epidermal cells (purple) and AIY at zone 2 synapses (green, note vesicles and dense projections in the two AIY-neurite cross sections). The dashed box in the schematic of the worm head represents the region where images (and schematic illustrations) in (B)–(Q) were obtained. The electron micrograph is from animals “JSH” and (legend continued on next page)

(Cox and Hirsh, 1985; Liu and Ambros, 1991). We observed significant rescue of the AIY presynaptic defect, consistent with *cima-1* playing a postdevelopmental role in epidermal cells to maintain synaptic distribution (Figure S3I).

### The *cima-1* Phenotype Is Affected by Animal Size

Animals increase their size after concluding larval development. To examine if *cima-1* is required to maintain synaptic positions during postdevelopmental growth, we visualized mutants that have abnormally short (dumpy or *Dpy*) or long (*Lon*) body length (Figures S5A–S5C; Page and Johnstone, 2007). The presynaptic pattern in *Dpy* animals retained a wild-type distribution in AIY (data not shown). Similarly, *lon-3(e2175)* animals display a longer synaptic region in AIY, but their synaptic distribution does not phenocopy *cima-1* (Figures S5C, S5F, and S5J). However, *cima-1(wy84)lon-3(e2175)* double mutants display a significantly enhanced AIY presynaptic maintenance defect (Figures S5I and S5J). Importantly, the enhancement of the presynaptic distribution phenotype in *cima-1(wy84)lon-3(e2175)* double mutants was observed after late L4 stage (data not shown). Moreover, *cima-1(wy84)dpy-4(e1166)* double mutants suppressed the *cima-1(wy84)* AIY presynaptic defect (Figure S5E). This suppression is likely due to the shorter size of the animal, as a number of *Dpy* alleles with different genetic identities gave us the same result (*dpy-7(e88)*, *dpy-9(e12)*, and *dpy-6(e14)*) (Figure S5H and data not shown). Together, our findings support a role for *cima-1* in maintaining presynaptic distribution during postdevelopmental growth.

### *cima-1* Is Required for Maintenance of Glial Morphology during Growth

The ventral cephalic sheath cells (VCSC) are nonneuronal cells (glia) similar to vertebrate astrocytes and are sandwiched between the *cima-1*-expressing *hyp7* epidermal cell and the AIY interneurons (Figure 5A and Shaham, 2006; White et al., 1986). To visualize these glial cells, we expressed cytoplasmic mCherry using the glia-specific *hlh-17* promoter (McMiller and Johnson, 2005).

In wild-type animals, VCSC glia are in close proximity to AIY zone 2 but are never observed near the asynaptic zone 1 (Figures 5B–5E). In larval stages, *cima-1(wy84)* VCSC morphology is indistinguishable from that of wild-type animals (Figures 5F–5I). However, in adult stages, the glial processes (endfeet) were abnormally distended posteriorly onto zone 1 of AIY (Figures 5J–5M). Cell-specific expression of *cima-1* in epidermal cells was sufficient to rescue the glial morphology (Figures 5N–5Q). Thus, *cima-1* is required in epidermal cells for maintenance of glial morphology during postlarval growth.

Does position of the glial endfeet correlate with the emergence of ectopic synaptic sites? To address this question, we conducted longitudinal studies and observed a tight temporal and spatial correlation between the position of the glial endfeet and the position of AIY presynaptic sites (Figure S6). Our findings indicate that *cima-1* acts in epidermal cells to maintain VCSC glial morphology during postlarval growth and reveal a correlation between the defective maintenance of glial morphology and the emergence of ectopic presynaptic sites in AIY.

### Glial Cell Ablation Suppresses Ectopic Synaptic Sites in *cima-1* Mutants

Our findings are consistent with a model in which distended glial endfeet in *cima-1(wy84)* mutants result in ectopic contact between glia and AIY, which in turn induces the formation of ectopic synaptic sites. To examine this hypothesis, we performed GFP reconstitution across synaptic partners (GRASP) between glia and AIY (Feinberg et al., 2008). We expressed CD4::GFP 11 in AIY and CD4::GFP 1–10 in glia to examine sites of AIY:glia contact. Consistent with published EM data (Figures S1A–S1B and White et al., 1986), we observed that in wild-type animals the GRASP signal was restricted to zone 2 and colocalized with the synaptic marker mCherry::RAB-3 (Figures 6A–6C). *cima-1(wy84)* mutant animals displayed an ectopic GRASP signal in zone 1 that colocalized with the ectopic mCherry::RAB-3 (Figures 6D–6F). Our findings suggest that ectopic AIY:glia contact in *cima-1(wy84)* mutant animals results in ectopic presynaptic specializations (Figures 6E and 6F).

To test whether glia:AIY contact is required for ectopic synapse formation, we ablated VCSC in two ways. First, we genetically ablated the glia by expressing caspases in these cells (Chelur and Chalfie, 2007). The cell death was confirmed by the absence of VCSC GFP. We observed that cell-specific ablation of the glia in *cima-1(wy84)* mutants significantly suppressed ectopic presynaptic sites in zone 1 (Figures 6H and 6I). Second, we examined the AIY presynaptic pattern in *cima-1(wy84)mls-2(ns156)* double mutants. *mls-2* is a transcription factor required for VCSC development, and in *mls-2(ns156)* mutant animals the glia do not properly develop (Yoshimura et al., 2008). Consistent with caspase ablation results, we also observed that ectopic presynaptic sites in zone 1 are suppressed in *cima-1(wy84)mls-2(ns156)* double mutant animals (Figures 6I). It should be noted, however, that loss of the glia in these experiments did not fully suppress the *cima-1* phenotype. Incomplete suppression could result from two possibilities: (1) caspase and genetic ablations do not completely eliminate the glia, or (2) other tissues besides VCSC glia also influence the persistence of ectopic presynaptic sites in AIY.

“N2U” shown with permission, each was prepared by J. White, E. Southgate, N. Thomson, and S. Brenner at the LMB/MRC labs in Cambridge, England (White et al., 1986). With help from John White, the JSH and N2U image archives are now conserved in the Hall lab in NYC, and available online at <http://www.wormimage.org>. Schematic illustration is a modification with permission from the Neuron pages of WormAtlas (<http://www.wormatlas.org>) by Z.F. Altun and D.H. Hall.

(B–Q) Simultaneous visualization of AIY presynaptic sites (green) and VCSC glia (red) in wild-type adult animal (B–D), *cima-1(wy84)* L4 animal (F)–(H), *cima-1(wy84)* adult animal (J)–(L), or *cima-1(wy84)* adult animal rescued with *Pdpy-4::cima-1* (N)–(P). Images (D), (H), (L), and (P) are as (C), (G), (K), and (O), but overlaid with DIC. Note that in *cima-1(wy84)* adult animals, VCSC glia abnormally distend to the zone 1 region and overlap with AIY ectopic presynapses (dashed box; [J]–[M]). Both glia and AIY presynaptic defects are rescued by expressing *cima-1* cDNA in epidermal cells (N)–(Q). In all images, white and black asterisk represent the location of the AIY cell body, and orange asterisks mark pharyngeal grinder. Note that in K and L, synapses are formed in zone 1, past the orange asterisk. (E), (I), (M), and (Q) are cartoons of (D), (H), (L), and (P) with pharynx in gray (see schematic in [A]). The *hlh-17* promoter labels both dorsal and ventral glial cells. The dorsal glia not labeled in (K) and (L) is due to the mosaic retention of the transgenic marker.

Scale bar in (B) corresponds to 10  $\mu$ m and applies to all images. See also Figure S6.

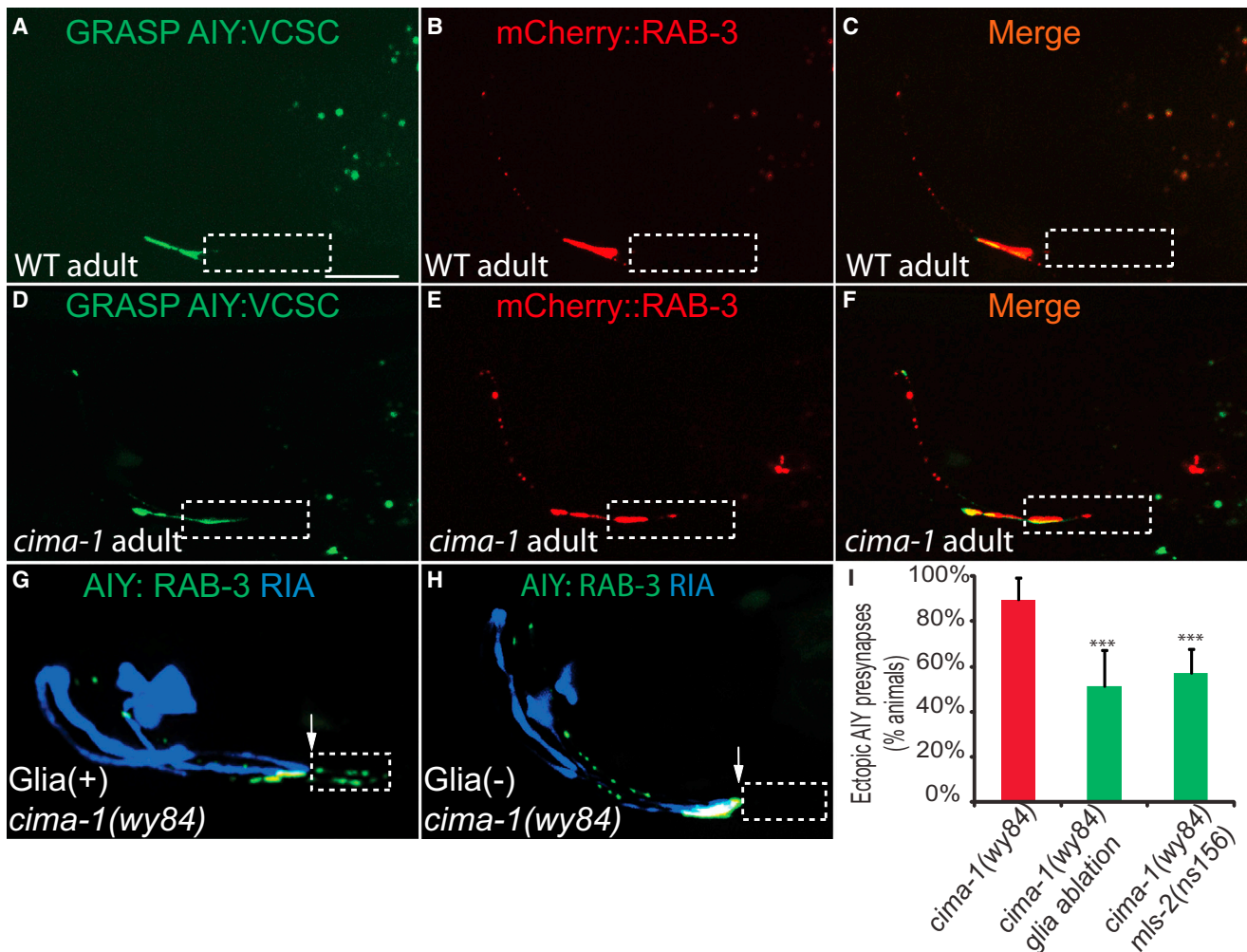


**Figure 6. VCSC Glia Abnormally Contact AIY and Are Required for Formation of Ectopic Presynaptic Sites in Zone 1 in *cima-1(wy84)*.**

(A–F) Simultaneous visualization of GRASP GFP signal (which indicates contact between AIY and VCSC glia) (A, D) and mCherry::RAB-3 (B) and (E)) in wild-type (A)–(C) and *cima-1(wy84)* (D)–(F) adult animals. Note that in *cima-1(wy84)* mutants VCSC glia abnormally contact AIY in zone 1 (indicated by GRASP GFP in dashed box), and that these sites correlate with sites of ectopic mCherry::RAB-3 in zone 1.

(G) In *cima-1(wy84)* adult animals, AIY forms ectopic presynaptic sites in zone 1 (dashed box) beyond zone 2 (determined by the position of postsynaptic partner RIA in blue). Arrow indicates the end of zone 2 and the beginning of zone 1.

(H) As in (G), but with VCSC genetically ablated through the cell-specific expression of caspases. Note suppression of ectopic presynaptic sites in zone 1 (dashed box).

(I) Quantification of the percentage of animals displaying ectopic presynaptic sites in zone 1 in *cima-1(wy84)* adult mutants; in *cima-1(wy84)* adult mutants expressing caspases cell specifically in VCSC glia, or in *cima-1(wy84)* *mls-2(ns156)* double mutants.

The scale bar in (A) is 10  $\mu$ m and applies to (A)–(H).  $n \geq 37$  for each genotype. Error bars represent 95% confidence interval. \*\*\* $p < 0.001$  between groups as determined by Fisher's exact test. See also Figure S1.

Together, these data suggest that epidermally expressed *cima-1* regulates glial morphology during postlarval growth and that maintenance of correct glial morphology during growth is required for preventing the emergence of ectopic presynaptic sites in AIY.

#### Ectopic Synapses Do Not Require Embryonic Specification Genes

During embryogenesis, AIY synapse formation requires UNC-6/Netrin, which is transiently expressed by VCSC glia (Colón-

Ramos et al., 2007; Wadsworth et al., 1996). UNC-6 instructs presynaptic assembly by signaling through its receptor UNC-40/DCC, expressed in AIY. We used the Netrin receptor, UNC-40, to test whether Netrin signaling is required for the *cima-1* mutant phenotype. To achieve this, we generated *cima-1(wy84)* *unc-40(e271)* double mutants and visualized the AIY presynaptic pattern. In juvenile worms, we observed a general reduction of presynaptic vesicle clusters in *cima-1(wy84)* *unc-40(e271)* compared to wild-type animals, as expected (Figure S7H and Colón-Ramos et al., 2007). In adults, *cima-1(wy84)*

*unc-40(e271)* animals still displayed ectopic presynaptic sites in zone 1 similar to *cima-1(wy84)* single mutants (Figures S7A–S7G). These findings suggest that VCSC glia use different molecular mechanisms for presynaptic assembly during embryonic development and for the maintenance of presynaptic distribution during postdevelopmental growth.

### EGL-15(5A)/FGFR Is Required for Ectopic Synapse Formation

To understand the molecular mechanisms by which *cima-1* affects AIY presynaptic maintenance during postlarval growth, we conducted candidate suppressor screens using RNAi and available mutants. These genetic approaches revealed that mutations of *egl-15*, the only FGFR in *C. elegans*, suppress the *cima-1* AIY presynaptic defect (Figures 7A, 7B, and 7C, and S7I;  $n > 300$  animals).

*egl-15/FGFR* is required during *C. elegans* development for sex myoblast migration, axon outgrowth, and fluid homeostasis, and null alleles of *egl-15* are larval lethal (Bülow et al., 2004; Goodman et al., 2003). Splicing isoform *egl-15(5A)*, but not isoform *egl-15(5B)*, is also required postembryonically to maintain axon position during growth and movement (Bülow et al., 2004). We observed that *egl-15(n484)*, a nonsense allele specific to the *egl-15(5A)* isoform, suppressed *cima-1(wy84)* ectopic presynaptic sites (Figures 7A, 7B, and S7I). Similarly, *egl-15(ay1)*, an *egl-15(5A)* splicing acceptor mutation (Goodman et al., 2003), also suppressed *cima-1(wy84)* AIY ectopic synapses (Figures 7C and S7I). These data demonstrate that the formation of ectopic presynaptic sites in *cima-1* mutants requires *egl-15(5A)*.

We next examined VCSC glial morphology in *cima-1(wy84)* *egl-15(n484)* double mutants. We observed that *egl-15(n484)* also suppresses the abnormal glial morphology observed in *cima-1(wy84)* mutants (Figures 7D and 7E). Consistent with this observation, glia ablation did not enhance suppression of the *cima-1(wy84)* *egl-15(n484)* double mutants (Figure S7I). Our data suggest that *egl-15(n484)* suppresses the AIY presynaptic defect by suppressing abnormal VCSC glial morphology in *cima-1(wy84)* mutants.

### EGL-15(5A)/FGFR Acts in the Epidermis Independent of Kinase Activity

Expression of *egl-15(5A)* cDNA using a pan-neuronal promoter did not restore ectopic presynapses to *egl-15(n484)* *cima-1(wy84)* double mutants. However, expression of *egl-15(5A)* in epidermal cells restored ectopic presynapses to *egl-15(n484)* *cima-1(wy84)* double mutants (Figures 7F and S7I), suggesting that FGFR isoform 5A, like *cima-1*, acts in the epidermal cells.

EGL-15 is a receptor tyrosine kinase activated by FGF ligands, which activates downstream Ras pathways (Borland et al., 2001; Sundaram, 2006); kinase activity is required by EGL-15(5B) to regulate axon outgrowth and fluid homeostasis (Bülow et al., 2004; Goodman et al., 2003; Huang and Stern, 2004). However, EGL-15(5A) does not require the intracellular kinase domain to maintain axon positions (Bülow et al., 2004). Similarly, we found that neither *egl-17(ay6)* nor *let-756(s2613)* suppress the presynaptic phenotype in *cima-1(wy84)* mutants (data not shown),

suggesting that FGF ligands, *egl-17* and *let-756*, are not required for ectopic presynapse formation in *cima-1* mutants.

To further test whether the kinase domain of EGL-15(5A) is required for the formation of ectopic synapses, we expressed the previously described *egl-15(5A)* extracellular domain (“*egl-15(5A)ecto*”; Bülow et al., 2004) in the epidermal cells in *egl-15(n484)* *cima-1(wy84)* double mutant animals, and found that expression of the ectodomain reverted *egl-15(n484)* suppression of *cima-1(wy84)* (Figure S7I). Together, these findings indicate that *egl-15(5A)* is required in epidermal cells in a kinase-independent manner to distort glial morphology in *cima-1* mutants.

### CIMA-1 Negatively Regulates EGL-15(5A)/FGFR Protein Levels

To determine how *cima-1* acts in epidermal cells to maintain presynaptic positions, we first examined its subcellular localization. We observed that CIMA-1::RFP is largely colocalized with lysosomal marker GFP::CUP-5 (Figures S3V–S3Y, Pearson's correlation = 0.53), suggesting that CIMA-1 localizes primarily to lysosomes. However, alleles that disrupt lysosomal function (such as *glo-1(zu391)*, *glo-4(ok623)*, *rab-7(ok511)*, and *cup-5(ar465)*) did not phenocopy *cima-1(wy84)* (data not shown). Our findings suggest that the *cima-1* phenotype does not result from general lysosomal dysfunction.

CIMA-1 localization is reminiscent of that seen for sialin, a vertebrate homolog of CIMA-1 that also localizes to lysosomes and vesicles and that in humans is associated with neurodegenerative disease (Verheijen et al., 1999). Sialin regulates transmembrane and extracellular adhesion molecules (Galuska et al., 2010; Hildebrandt et al., 2009; Morin et al., 2004; Myall et al., 2007; Prolo et al., 2009; Verheijen et al., 1999). Based on CIMA-1 localization, and its genetic interaction with EGL-15(5A), we hypothesized that CIMA-1 could be acting at the lysosome to regulate EGL-15(5A) in epidermal cells. To examine this hypothesis, we generated transgenic animals expressing C terminus HA-tagged EGL-15(5A) just in epidermal cells and probed protein levels by western blots in both *cima-1(wy84)* and wild-type animals. We consistently found that EGL-15(5A) levels are 5-fold higher in *cima-1(wy84)* animals than in wild-type animals (Figures 7G and 7H,  $p = 0.007$ ). This result suggests that *cima-1* is required for the regulation of EGL-15(5A) protein levels in epidermal cells.

To further test whether the synaptic defect in *cima-1* is due to the increase of EGL-15(5A) in epidermal cells, we generated transgenic lines overexpressing EGL-15(5A) in epidermal cells and observed that overexpression of EGL-15(5A) in wild-type animals resulted in abnormal glial morphology and ectopic presynaptic specializations in zone 1, similar to the phenotypes observed for *cima-1(wy84)* mutants (Figures 7I–7K). Together, our findings support a model whereby the transporter *cima-1* maintains glial morphology and presynaptic distribution by negatively regulating EGL-15(5A)/FGFR during growth. We hypothesize that reduction of EGL-15(5A) levels would result in reduced adhesion between glia and epidermal cells, which would be critical in maintaining glia location and, therefore, synapse location during postdevelopmental growth.

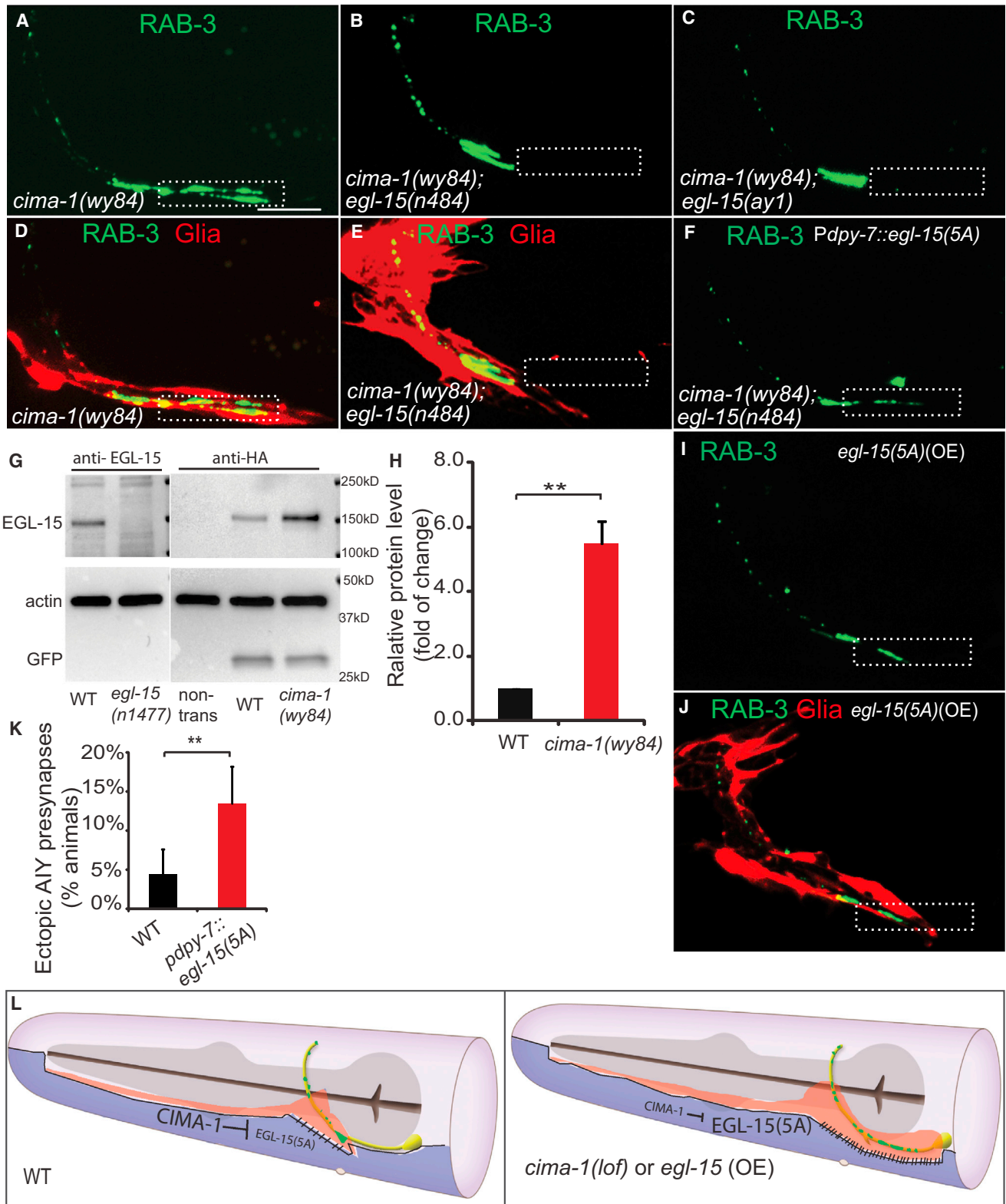


**Figure 7. *egl-15/fgfr* Is Required for Ectopic Synapse Formation in *cima-1(wy84)* Animals**

(A–C) GFP::RAB-3 in *cima-1(wy84)* mutant (A), *cima-1(wy84) egl-15(n484)* double mutant (B) and *cima-1(wy84) egl-15(ay1)* double mutant (C) adult animals. Note that alleles *egl-15(n484)* and *egl-15(ay1)*, which specifically disrupt *egl-15(5A)* isoform, suppress *cima-1(wy84)* presynaptic distribution defect.

(legend continued on next page)

## DISCUSSION

In this study, we identify a cellular and molecular mechanism that maintains presynaptic distribution during *C. elegans* postdevelopmental growth. We uncovered the requirement of a SLC17 family transporter CIMA-1. CIMA-1 antagonizes a specific FGFR isoform, EGL-15(5A), in epidermal cells to modulate glial morphology, in turn modulating AIY synaptic distribution.

CIMA-1 acts postdevelopmentally to regulate synaptic positions during growth. Between the L1 to L4 stage, animals undergo a 4-fold change in length. However, during these stages, *cima-1* mutants resemble wild-type animals. We hypothesize that *cima-1*-independent mechanisms scale synaptic growth during development and that *cima-1* is required to regulate synaptic positions during postdevelopmental growth. Two lines of evidence support this hypothesis. First, *cima-1* expression after larval stages using the *col-19* promoter rescues the presynaptic distribution phenotype in AIY. Second, in the *cima-1* mutant background, Lon mutants display an enhanced presynaptic maintenance phenotype and Dpy mutants suppress the *cima-1* phenotype. These findings demonstrate a relationship between animal size and the postdevelopmental expressivity of the *cima-1* phenotype and indicate a role for *cima-1* in maintenance of the synaptic pattern during postdevelopmental growth.

*cima-1* negatively regulates an FGFR isoform, *egl-15(5A)*, to modulate glial morphology during growth. Four lines of evidence support this model. First, like *cima-1*, *egl-15(5A)* is also expressed, and required, in epidermal cells to modulate epidermal-glia interaction. Second, in the epidermal cells of *cima-1* mutant animals, EGL-15(5A) protein levels are significantly increased. Third, loss of *egl-15(5A)* in *cima-1* mutants mostly restores glial morphology and correct presynaptic patterning in AIY. Fourth, overexpression of *egl-15(5A)* in wild-type animals results in abnormally extended glia and in ectopic presynaptic sites in AIY. EGL-15(5A) was previously implicated in the maintenance of axon position in the ventral nerve cord (Bülow et al., 2004). This function of EGL-15(5A) is also mediated by its ecto-domain, which was hypothesized to provide an adhe-

sive substratum as a part of a larger adhesive complex (Benard and Hobert, 2009; Bülow et al., 2004). Our findings now demonstrate that CIMA-1 can negatively regulate EGL-15(5A) to maintain glial morphology during growth.

CIMA-1 could act as a sugar transporter to regulate EGL-15(5A) protein levels. CIMA-1 is a member of the solute carrier SLC17 family that includes sialin. Although sialin is capable of transporting a variety of cargos depending on its biological context (Miyaji et al., 2010, 2011; Qin et al., 2012), its role as a lysosomal transporter of acidic monosaccharides has been implicated in neurological diseases (Verheijen et al., 1999; Wreden et al., 2005). Importantly, several studies suggest that sialin regulates intercellular adhesion via the modulation of glycoconjugate export from the lysosome (Galuska et al., 2010; Hildebrandt et al., 2009; Morin et al., 2004; Myall et al., 2007; Prolo et al., 2009). CIMA-1 also localizes to the lysosome. Although we have not yet identified the specific cargo for CIMA-1, our phenotypic characterization uncovers an *in vivo* function for this transporter in maintaining presynaptic distribution by regulating specific isoform of the FGFR, EGL-15(5A). EGL-15 is N-glycosylated (Polanska et al., 2009). We hypothesize that CIMA-1 could act like sialin in transporting acidic monosaccharides that could modify and regulate protein levels of EGL-15(5A). Although our findings are consistent with this hypothesis and demonstrate a genetic interaction between *cima-1* and EGL-15(5A) *in vivo*, it is likely that *cima-1* also regulates other molecules, as mutations of *egl-15(5A)* do not completely suppress the *cima-1* phenotype.

The role of glia in synapse formation and function is well-established. In both vertebrates and invertebrates, glia-derived molecules promote synapse formation during development (Allen et al., 2012; Colón-Ramos et al., 2007; Fuentes-Medel et al., 2012; Pfrieger, 2010; Stevens, 2008). Glia are also required *in vivo* for maintenance of synaptic function in adult animals. For example, ablation of glia in adult *Rana pipiens* decreases presynaptic function at neuromuscular junctions (Reddy et al., 2003). Although glia are known to play roles in maintenance of synaptic function, their role in maintenance of synaptic positions is less

(D–E) Simultaneous visualization of presynaptic sites in AIY (green) and glia (red) in *cima-1(wy84)* (D) and *cima-1(wy84) egl-15(n484)* double mutant adult animals (E). Note that *egl-15(n484)* allele suppresses both the AIY presynaptic defect and the glia morphology defect in *cima-1(wy84)*.

(F) Expression of *egl-15(5A)* cDNA in the epidermal cells (using the *dpy-7* promoter) reverts the suppression of the *cima-1(wy84)* AIY presynaptic phenotype by *egl-15(n484)*.

(G) EGL-15 crackle antibody (a gift from M Stern), detects endogenous EGL-15, the 141 kD band in wild-type (lane 1), but not in *egl-15(n1477)* mutants (lane 2), which produced the C terminus truncated EGL-15 (M Stern, personal communication). HA antibody specifically recognizes HA-tagged EGL-15(5A) expressed in epidermal cells (lane 4 and 5), but not in wild-type animals without the transgene (lane 3). For comparison in lanes 4 and 5, the same HA-tagged EGL-15(5A)-expressing transgenic line were used. Note that EGL-15(5A) protein levels are higher in *cima-1(wy84)* mutant animals (lane 5) as compared to wild-type animals (lane 4). Actin and coinjection marker *Punc-122::GFP* were used as loading control.

(H) Quantification of the EGL-15(5A)::HA protein levels from four independent blots. Error bars are SEM, \*\**p* < 0.01 by Student's *t* test.

(I–J) AIY presynaptic GFP::RAB-3 (I) is mislocalized to zone 1 region abnormally ensheathed by VCSC (J) upon overexpression of *egl-15(5A)* in epidermal cells by using the *dpy-7* promoter (compare to Figure 5C).

(K) Quantification of the percentage of animals with the phenotype shown in (I). *n* ≥ 150 for each group. Error bars represent 95% confidence interval. \*\**p* < 0.01 groups as determined by Fisher's exact test.

(L) A model for *cima-1* and *egl-15(5A)* in epidermal cells (purple) regulating VCSC glia (red) morphology and AIY presynaptic distribution (green). In wild-type animals, *cima-1* negatively regulates *egl-15(5A)*, thereby reducing epidermal-glia adhesion and preventing glia extension during growth. This interaction contributes to maintaining wild-type VCSC morphology, which in turn specifies correct synaptic distribution during growth (left cartoon). In animals with *cima-1* loss-of-function, or animals in which *egl-15(5A)* is overexpressed, the interaction between the epidermal cells and VCSC is misregulated, resulting in VCSC glia distension posteriorly, ectopic contacts between glia and axons, and ectopic presynaptic sites. Schematic illustration is a modification with permission from the Neuron pages of WormAtlas (<http://www.wormatlas.org>) by Z.F. Altun and D.H. Hall.

See also Figure S7.

clear. A recent study demonstrates that growth of glial processes is coordinated with neuromuscular junction growth in vivo (Brink et al., 2012). We show a postdevelopmental role for glia in maintaining synaptic distribution and circuit architecture during growth.

The transduction of growth information from epithelial cell, to glia, to neuron may be common. The epidermal epithelium in *C. elegans* coordinates growth in the organism. For example, genes expressed in epidermal cells regulate molting, body morphogenesis and animal size (Chisholm and Hardin, 2005; Chisholm and Hsiao, 2012; Chisholm and Xu, 2012). Our work shows that the interaction of epidermal cells with glia translates growth information to the neurons to limit synapse distribution. The epithelial-glia interaction we uncovered here is reminiscent of the neurovascular unit in vertebrates. Astrocytes play a fundamental role mediating communication between epithelial cells and neurons in the vasculature of the brain (Abbott et al., 2006; Banerjee and Bhat, 2007; Giaume et al., 2010; Kim et al., 2006; Tam and Watts, 2010; Wolburg et al., 2009). For example, astrocytes indirectly control blood flow to neurons by coupling neuronal activity to the epithelial cells of the vasculature (Allan, 2006; Koehler et al., 2009). Astrocytes also developmentally couple epithelial cells of the vasculature with neurons during embryogenesis (Tam and Watts, 2010). It is not yet known if astrocytes translate growth information from epithelial cells in the vasculature to position synapses as the animal grows. However, given existing roles for astrocytes in coupling functional and developmental information between epithelial cells and neurons, we speculate that analogous, glia-dependent mechanisms like those in *C. elegans* could maintain synaptic position during animal growth in metazoans.

## EXPERIMENTAL PROCEDURES

For further experimental details on strains (Table S1), culture conditions, and statistics, please see the Extended Experimental Information.

### EMS Screen and RNAi

*cima-1(wy84)* was isolated from a visual forward EMS mutagenesis screen aimed at identifying mutants with defects in GFP::RAB-3 distribution. *cima-1* was mapped to an interval between 7.40 Mb and 7.83 Mb on chromosome IV. The 18 fosmids that cover this region were injected into *cima-1(wy84)* mutants and examined for rescue of AIY presynaptic defects. The F45E4.11 region in *cima-1(wy84)* was sequenced with Sanger sequencing technique. Bacteria-mediated RNAi was performed as described in (Kamath et al., 2001).

### Constructs and Nematode Transformation

Expression clones were made in the pSM vector, a derivative of pPD49.26 (A. Fire) with extra cloning sites. Constructs are listed in Table S2, and detailed cloning information will be provided upon request. Transgenic strains (1–30 ng/ $\mu$ l) were generated using standard techniques (Mello and Fire, 1995) and listed in Table S2.

### Microscopy and Imaging

*C. elegans* animals (*cima-1(wy84)*, *Pttx-3::GFP*) were prepared for fluorescence electron microscopy as previously described (Watanabe et al., 2011). AIY neurons in two *cima-1(wy84)* animals were identified based on fluorescence. Fluorescence images and electron micrographs were correlated based on the fiducial markers. Epidermal and VCSC glial cells were identified based on their morphology. A total length of 6  $\mu$ m of an AIY and a VCSC glial cell were reconstructed from serial electron micrographs as shown in Figure S1F. Reconstruction of AIY and glia in the wild-type animal used EM images (JSH and N2U)

prepared by Dr. John White (White et al., 1986), downloaded from <http://www.wormimage.org> and reconstructed with TrakEM2 EM. For confocal microscopy, images of fluorescently tagged fusion proteins were captured in live *C. elegans* using an UltraView VoX spinning disc confocal microscope (PerkinElmer) as described and analyzed using Velocity software (Improvision) or ImageJ (Schneider et al., 2012; Stavoe and Colón-Ramos, 2012).

### Protein Blots

We quantified EGL-15::HA in wild-type and *cima-1(wy84)* mutant animals using *olaEx1288 (Pdpi-7::egl-15(5A)::HA::MYC)*. 40–60 transgenic L4 animals were used for the blots. Reagents and detailed procedures are in the Extended Experimental Procedures section. This experiment was repeated four times with similar results. We also performed an identical experiment with a second, independent transgenic strain (*olaEx1411*) and three replicated western blots with similar results.

## SUPPLEMENTAL INFORMATION

Supplemental Information includes Extended Experimental Procedures, seven figures, and two tables and can be found with this article online at <http://dx.doi.org/10.1016/j.cell.2013.06.028>.

## ACKNOWLEDGMENTS

Some illustrations were created by Z.F. Altun and D.H. Hall from WormAtlas. The EM in Fig 5A, Fig S1C and S1D were prepared by J. White, E. Southgate, N. Thomson and S. Brenner at the LMB/MRC labs in Cambridge, England (White et al., 1986). The adult image in the graphical abstract was created by Dr. Maria Gallegos of Cal State University. We thank Dr. H. Bülow, Dr. M. Stern, Dr. S. Shaham, Dr. T. Kinnunen, Dr. J. Fares, Dr. K. Shen, and CGC for strains and reagents. We also thank A. Pérez and A. Roque for technical assistance, Dr. X. Song for helping with the protein blots, and D. Hall, S. Margolis, P. De Camilli, S. Strittmatter, M. Hammarlund, and members of the Colón-Ramos lab for helpful discussions and sharing of advice. This work was funded by the following grants to D.C.-R. (R00 NS057931, R01 NS076558, a fellowship from the Klingenstein Foundation and the Alfred P. Sloan Foundation and a March of Dimes Research Grant) and to E.M.J. (NIH R01 NS034307, NSF 0920069). E.M.J. is an Investigator of the Howard Hughes Medical Institute. Z.S. and D.A.C.-R. designed experiments. S.W. and E.M.J. performed the fEM experiments. R. C. performed wild type EM reconstruction and AIY Zone 1 length quantification. Z.S. performed all other experiments. Z.S. and D.A.C.-R. analyzed and interpreted the data. Z.S., S.W., E.M.J., and D.A.C.-R. wrote the paper.

Received: November 3, 2012

Revised: April 9, 2013

Accepted: June 19, 2013

Published: July 18, 2013

## REFERENCES

- Abbott, N.J., Ronnback, L., and Hansson, E. (2006). Astrocyte-endothelial interactions at the blood-brain barrier. *Nat. Rev. Neurosci.* 7, 41–53.
- Allan, S. (2006). The neurovascular unit and the key role of astrocytes in the regulation of cerebral blood flow. *Cerebrovasc. Dis.* 21, 137–138.
- Allen, N.J., Bennett, M.L., Foo, L.C., Wang, G.X., Chakraborty, C., Smith, S.J., and Barres, B.A. (2012). Astrocyte glypicans 4 and 6 promote formation of excitatory synapses via GluA1 AMPA receptors. *Nature* 486, 410–414.
- Aurelio, O., Hall, D.H., and Hobert, O. (2002). Immunoglobulin-domain proteins required for maintenance of ventral nerve cord organization. *Science* 295, 686–690.
- Banerjee, S., and Bhat, M.A. (2007). Neuron-glia interactions in blood-brain barrier formation. *Annu. Rev. Neurosci.* 30, 235–258.
- Benard, C., and Hobert, O. (2009). Looking beyond development: maintaining nervous system architecture. *Curr. Top. Dev. Biol.* 87, 175–194.

- Benard, C.Y., Boyanov, A., Hall, D.H., and Hobert, O. (2006). DIG-1, a novel giant protein, non-autonomously mediates maintenance of nervous system architecture. *Development* 133, 3329–3340.
- Benard, C.Y., Blanchette, C., Recio, J., and Hobert, O. (2012). The Secreted Immunoglobulin Domain Proteins ZIG-5 and ZIG-8 Cooperate with L1CAM/SAX-7 to Maintain Nervous System Integrity. *PLoS Genet.* 8, e1002819.
- Borland, C.Z., Schutzman, J.L., and Stern, M.J. (2001). Fibroblast growth factor signaling in *Caenorhabditis elegans*. *Bioessays* 23, 1120–1130.
- Brenner, S. (1974). The genetics of *Caenorhabditis elegans*. *Genetics* 77, 71–94.
- Brink, D.L., Gilbert, M., Xie, X., Petley-Ragan, L., and Auld, V.J. (2012). Glial processes at the *Drosophila* larval neuromuscular junction match synaptic growth. *PLoS ONE* 7, e37876.
- Bülöw, H.E., Boulin, T., and Hobert, O. (2004). Differential functions of the *C. elegans* FGF receptor in axon outgrowth and maintenance of axon position. *Neuron* 42, 367–374.
- Chelur, D.S., and Chalfie, M. (2007). Targeted cell killing by reconstituted caspases. *Proc. Natl. Acad. Sci. USA* 104, 2283–2288.
- Chisholm, A.D., and Hardin, J. (2005). Epidermal morphogenesis. In *WormBook, The C. elegans Research Community*, ed. <http://dx.doi.org/10.1895/wormbook.1.35.1>, <http://www.wormbook.org>.
- Chisholm, A.D., and Hsiao, T.I. (2012). The *Caenorhabditis elegans* epidermis as a model skin. I: development, patterning, and growth. *Wiley Interdiscip Rev Dev Biol.* 1, 861–878.
- Chisholm, A.D., and Xu, S. (2012). The *Caenorhabditis elegans* epidermis as a model skin. II: differentiation and physiological roles. *Wiley Interdiscip Rev Dev Biol.* 1, 879–902.
- Colón-Ramos, D.A., Margeta, M.A., and Shen, K. (2007). Glia promote local synaptogenesis through UNC-6 (netrin) signaling in *C. elegans*. *Science* 318, 103–106.
- Cox, G.N., and Hirsh, D. (1985). Stage-specific patterns of collagen gene expression during development of *Caenorhabditis elegans*. *Mol. Cell. Biol.* 5, 363–372.
- Feinberg, E.H., Vanhoven, M.K., Bendesky, A., Wang, G., Fetter, R.D., Shen, K., and Bargmann, C.I. (2008). GFP Reconstitution Across Synaptic Partners (GRASP) defines cell contacts and synapses in living nervous systems. *Neuron* 57, 353–363.
- Fuentes-Medel, Y., Ashley, J., Barria, R., Maloney, R., Freeman, M., and Budnik, V. (2012). Integration of a Retrograde Signal during Synapse Formation by Glia-Secreted TGF-beta Ligand. *Curr. Biol.* 22, 1831–1838.
- Galuska, S.P., Rollenhagen, M., Kaup, M., Eggers, K., Oltmann-Norden, I., Schiff, M., Hartmann, M., Weinhold, B., Hildebrandt, H., Geyer, R., et al. (2010). Synaptic cell adhesion molecule SynCAM 1 is a target for polysialylation in postnatal mouse brain. *Proc. Natl. Acad. Sci. USA* 107, 10250–10255.
- Giaume, C., Koulakoff, A., Roux, L., Holcman, D., and Rouach, N. (2010). Astroglial networks: a step further in neuroglial and gliovascular interactions. *Nat. Rev. Neurosci.* 11, 87–99.
- Goodman, S.J., Branda, C.S., Robinson, M.K., Burdine, R.D., and Stern, M.J. (2003). Alternative splicing affecting a novel domain in the *C. elegans* EGL-15 FGF receptor confers functional specificity. *Development* 130, 3757–3766.
- Hildebrandt, H., Muhlenhoff, M., Oltmann-Norden, I., Rockle, I., Burkhardt, H., Weinhold, B., and Gerardy-Schahn, R. (2009). Imbalance of neural cell adhesion molecule and polysialyltransferase alleles causes defective brain connectivity. *Brain* 132, 2831–2838.
- Huang, P., and Stern, M.J. (2004). FGF signaling functions in the hypodermis to regulate fluid balance in *C. elegans*. *Development* 131, 2595–2604.
- Johnson, R.P., and Kramer, J.M. (2012). Neural maintenance roles for the matrix receptor dystroglycan and the nuclear anchorage complex in *Caenorhabditis elegans*. *Genetics* 190, 1365–1377.
- Kamath, R.S., Martinez-Campos, M., Zipperlen, P., Fraser, A.G., and Ahringer, J. (2001). Effectiveness of specific RNA-mediated interference through ingested double-stranded RNA in *Caenorhabditis elegans*. *Genome Biol* 2, RESEARCH0002.
- Kim, J.H., Park, J.A., Lee, S.W., Kim, W.J., Yu, Y.S., and Kim, K.W. (2006). Blood-neural barrier: intercellular communication at glio-vascular interface. *J. Biochem. Mol. Biol.* 39, 339–345.
- Knight, C.G., Patel, M.N., Azevedo, R.B., and Leroi, A.M. (2002). A novel mode of ecdysozoan growth in *Caenorhabditis elegans*. *Evol. Dev.* 4, 16–27.
- Koehler, R.C., Roman, R.J., and Harder, D.R. (2009). Astrocytes and the regulation of cerebral blood flow. *Trends Neurosci.* 32, 160–169.
- Lin, Y.C., and Koleske, A.J. (2010). Mechanisms of synapse and dendrite maintenance and their disruption in psychiatric and neurodegenerative disorders. *Annu. Rev. Neurosci.* 33, 349–378.
- Liu, Z., and Ambros, V. (1991). alternative temporal control systems for hypodermal cell differentiation in *Caenorhabditis elegans*. *Nature* 350, 162–165.
- McMiller, T.L., and Johnson, C.M. (2005). Molecular characterization of HLH-17, a *C. elegans* bHLH protein required for normal larval development. *Gene* 356, 1–10.
- Mello, C., and Fire, A. (1995). DNA transformation. *Methods Cell Biol.* 48, 451–482.
- Miyaji, T., Omote, H., and Moriyama, Y. (2010). A vesicular transporter that mediates aspartate and glutamate neurotransmission. *Biol. Pharm. Bull.* 33, 1783–1785.
- Miyaji, T., Omote, H., and Moriyama, Y. (2011). Functional characterization of vesicular excitatory amino acid transport by human sialin. *J. Neurochem.* 119, 1–5.
- Morin, P., Sagne, C., and Gasnier, B. (2004). Functional characterization of wild-type and mutant human sialin. *EMBO J.* 23, 4560–4570.
- Myall, N.J., Wreden, C.C., Wlizia, M., and Reimer, R.J. (2007). G328E and G409E sialin missense mutations similarly impair transport activity, but differentially affect trafficking. *Mol. Genet. Metab.* 92, 371–374.
- Nonet, M.L., Staunton, J.E., Kilgard, M.P., Fergestad, T., Hartwig, E., Horvitz, H.R., Jorgensen, E.M., and Meyer, B.J. (1997). *Caenorhabditis elegans* rab-3 mutant synapses exhibit impaired function and are partially depleted of vesicles. *J. Neurosci.* 17, 8061–8073.
- Page, A.P., and Johnstone, I.L. (2007). The cuticle. In *WormBook, The C. elegans Research Community*, ed. <http://dx.doi.org/10.1895/wormbook.1.138.1>, <http://www.wormbook.org>.
- Pfriege, F.W. (2010). Role of glial cells in the formation and maintenance of synapses. *Brain Res. Brain Res. Rev.* 63, 39–46.
- Pocock, R., Benard, C.Y., Shapiro, L., and Hobert, O. (2008). Functional dissection of the *C. elegans* cell adhesion molecule SAX-7, a homologue of human L1. *Mol. Cell. Neurosci.* 37, 56–68.
- Polanska, U.M., Duchesne, L., Harries, J.C., Fernig, D.G., and Kinnunen, T.K. (2009). N-Glycosylation regulates fibroblast growth factor receptor/EGL-15 activity in *Caenorhabditis elegans* in vivo. *J. Biol. Chem.* 284, 33030–33039.
- Prolo, L.M., Vogel, H., and Reimer, R.J. (2009). The lysosomal sialic acid transporter sialin is required for normal CNS myelination. *J. Neurosci.* 29, 15355–15365.
- Qin, L., Liu, X., Sun, Q., Fan, Z., Xia, D., Ding, G., Ong, H.L., Adams, D., Gahl, W.A., Zheng, C., et al. (2012). Sialin (SLC17A5) functions as a nitrate transporter in the plasma membrane. *Proc. Natl. Acad. Sci. USA* 109, 13434–13439.
- Reddy, L.V., Koirala, S., Sugiura, Y., Herrera, A.A., and Ko, C.P. (2003). Glial cells maintain synaptic structure and function and promote development of the neuromuscular junction in vivo. *Neuron* 40, 563–580.
- Reimer, R.J. (2013). SLC17: A functionally diverse family of organic anion transporters. *Mol. Aspects Med.* 34, 350–359.
- Sasakura, H., Inada, H., Kuhara, A., Fusaoka, E., Takemoto, D., Takeuchi, K., and Mori, I. (2005). Maintenance of neuronal positions in organized ganglia by SAX-7, a *Caenorhabditis elegans* homologue of L1. *EMBO J.* 24, 1477–1488.
- Schneider, C.A., Rasband, W.S., and Eliceiri, K.W. (2012). NIH Image to ImageJ: 25 years of image analysis. *Nat. Methods* 9, 671–675.

- Shaham, S. (2006). Glia-neuron interactions in the nervous system of *Caenorhabditis elegans*. *Curr. Opin. Neurobiol.* *16*, 522–528.
- Shi, L., Fu, A.K., and Ip, N.Y. (2012). Molecular mechanisms underlying maturation and maintenance of the vertebrate neuromuscular junction. *Trends Neurosci.* *35*, 441–453.
- Sreedharan, S., Shaik, J.H., Olszewski, P.K., Levine, A.S., Schioth, H.B., and Fredriksson, R. (2010). Glutamate, aspartate and nucleotide transporters in the SLC17 family form four main phylogenetic clusters: evolution and tissue expression. *BMC Genomics* *11*, 17.
- Stavoe, A.K., and Colón-Ramos, D.A. (2012). Netrin instructs synaptic vesicle clustering through Rac GTPase, MIG-10, and the actin cytoskeleton. *J. Cell Biol.* *197*, 75–88.
- Stevens, B. (2008). Neuron-astrocyte signaling in the development and plasticity of neural circuits. *Neurosignals* *16*, 278–288.
- Sulston, J.E., Schierenberg, E., White, J.G., and Thomson, J.N. (1983). The embryonic cell lineage of the nematode *Caenorhabditis elegans*. *Dev. Biol.* *100*, 64–119.
- Sundaram, M.V. (2006). RTK/Ras/MAPK signaling. In *WormBook, The C. elegans Research Community*, ed. <http://dx.doi.org/10.1895/wormbook.1.80.1>, <http://www.wormbook.org>.
- Tam, S.J., and Watts, R.J. (2010). Connecting vascular and nervous system development: angiogenesis and the blood-brain barrier. *Annu. Rev. Neurosci.* *33*, 379–408.
- Verheijen, F.W., Verbeek, E., Aula, N., Beerens, C.E., Havelaar, A.C., Joosse, M., Peltonen, L., Aula, P., Galjaard, H., van der Spek, P.J., et al. (1999). A new gene, encoding an anion transporter, is mutated in sialic acid storage diseases. *Nat. Genet.* *23*, 462–465.
- Wadsworth, W.G., Bhatt, H., and Hedgecock, E.M. (1996). Neuroglia and pioneer neurons express UNC-6 to provide global and local netrin cues for guiding migrations in *C. elegans*. *Neuron* *16*, 35–46.
- Watanabe, S., and Jorgensen, E.M. (2012). Visualizing proteins in electron micrographs at nanometer resolution. *Methods Cell Biol.* *111*, 283–306.
- Watanabe, S., Punge, A., Hollopeter, G., Willig, K.I., Hobson, R.J., Davis, M.W., Hell, S.W., and Jorgensen, E.M. (2011). Protein localization in electron micrographs using fluorescence nanoscopy. *Nat. Methods* *8*, 80–84.
- White, J.G., Southgate, E., Thomson, J.N., and Brenner, S. (1986). The Structure of the Nervous System of the Nematode *Caenorhabditis elegans*. *Philos. Trans. R. Soc. Lond. B Biol. Sci.* *314*, 1–340.
- Wilcox, K.C., Lacor, P.N., Pitt, J., and Klein, W.L. (2011). Abeta oligomer-induced synapse degeneration in Alzheimer's disease. *Cell. Mol. Neurobiol.* *31*, 939–948.
- Wolburg, H., Noell, S., Mack, A., Wolburg-Buchholz, K., and Fallier-Becker, P. (2009). Brain endothelial cells and the glio-vascular complex. *Cell Tissue Res.* *335*, 75–96.
- Woo, W.M., Berry, E.C., Hudson, M.L., Swale, R.E., Goncharov, A., and Chisholm, A.D. (2008). The *C. elegans* F-spondin family protein SPON-1 maintains cell adhesion in neural and non-neural tissues. *Development* *135*, 2747–2756.
- Wreden, C.C., Wlizla, M., and Reimer, R.J. (2005). Varied mechanisms underlie the free sialic acid storage disorders. *J. Biol. Chem.* *280*, 1408–1416.
- Yoshimura, S., Murray, J.I., Lu, Y., Waterston, R.H., and Shaham, S. (2008). *mls-2* and *vab-3* Control glia development, *hlh-17/Olig* expression and glia-dependent neurite extension in *C. elegans*. *Development* *135*, 2263–2275.

## EXTENDED EXPERIMENTAL PROCEDURES

### Strains

Worms were raised on NGM plates at 22°C using OP50 *E. coli* as a food source (Brenner, 1974). Strains used in this study were listed in Table S1.

### *cima-1(wy84)* Cloning

Fosmids injected for cloning *cima-1(wy84)* includes: WRM068bB06, WRM0617aA03, WRM0633-dE08, WRM0630bH07, WRM0618aA07, WRM067bC05, WRM0612aH07, WRM068aE11, WRM0616bG10, WRM066-dA02, WRM0623cD10, WRM0612BA03, WRM0615cC03, WRM0620cA08, WRM067aG11, WRM065aD01, WRM068-dD06, WRM0623cC07.

### Protein Blot

40–60 synchronized L4 animals were collected and boiled in 10 $\mu$ l M9 and 10 $\mu$ l 2x sample buffer (from Bio-Rad Life Science) for 10 min before loading to 4%–15% gradient polyacrylamide gels (from Bio-Rad Life Science). Blots were probed with monoclonal antibodies recognizing the following epitopes: GFP (HRP conjugated antibody from Cell Signaling at 1:500 dilution); HA (HRP conjugated antibody from Cell Signaling Technology clone 6E2 at 1:500 dilution); actin (HRP conjugated antibody from Santa Cruz Biotechnology at 1:10,000 dilution), or polyclonal anti-EGL-15 Crackle (a gift from M. Stern used at 1:1,000 dilution). The secondary antibody (HRP conjugated goat anti-rabbit antibody from Cell Signaling Technology) was diluted 1:2,000.

We used EGL-15 Crackle antibody (a gift from M Stern), which recognizes both isoform 5A and 5B expressed in all tissues (Lo et al., 2008). We observed that we could detect a 141 kDa protein band in wild-type animals (Figure 7G), but not in *egl-15(n1477)* or *egl-15(n1457)* mutants. *egl-15(n1477)* and *egl-15(n1457)* carry early stop at W878 and Q896, which produce the C terminus truncated EGL-15 that was not recognized by the antibody (Figure 7G, data not shown). These findings, which are consistent with unpublished protein characterizations, suggest that EGL-15 runs as a 141 kDa protein band (M Stern, personal communication). Then we examined the protein levels of the EGL-15(5A)-specific isoform in epidermal cells. To achieve this, we generated transgenic animals expressing C terminus HA-tagged EGL-15(5A) just in epidermal cells, and probed protein levels by western blots in both *cima-1(wy84)* and wild-type animals.

### Quantification and Statistics

For the AIY presynaptic pattern analyses, animals were synchronized at L1, L4 and adult stages. We calculated the ratio of the presynaptic region in a three-step process: First, we measured the length of the presynaptic region in the ventral part of the AIY neurite (zone 2 in wild-type animals, zone 2 and presynaptic zone 1 in *cima-1* mutants). Second, we measured the length of zone 3. Finally, we divided first measurement by total (measurement 1+2). The quantifications for the rescue experiments were done using a compound microscope (model DM5000 B; Leica). For each construct, multiple transgenic lines were generated and quantified. For quantifications of *cima-1(wy84)* suppression, animals were imaged using a confocal microscope. The AIY presynaptic pattern was scored as wild-type in confocal micrographs in which the AIY zone 2 presynaptic sites were located proximal to the RIA postsynaptic sites. In strains in which RIA was not imaged, we scored the zone 2 position as wild-type if it was located anterior to the pharyngeal grinder, or if its length was 11  $\mu$ m or shorter. VCSC glia ablation was performed by expressing caspase fragments cell specifically in cephalic sheath glia using the *hlh-17* promoter (Chelur and Chalfie, 2007; McMiller and Johnson, 2005; Yoshimura et al., 2008). An integrated cephalic sheath glial cytoplasmic GFP marker (Yoshimura et al., 2008) was used in the caspase transgenic lines to determine if VCSC glia were successfully ablated. Protein blot was quantified with Image Lab 4.1 (Bio-Rad). For each experiment, EGL-15::HA was normalized using actin intensity. The fold increase in *cima-1* mutant animals was established using wild-type as a baseline.

Statistical analyses regarding the presynaptic pattern distribution, tissue specific and fosmid rescue, AIY zone 1 length analyses, presynaptic puncta, intensity quantification, and protein levels were achieved using Student's t test. All other statistical analyses were done using Fisher's exact test.

### Constructs

pTB84 (*pdpy-7::egl-15(5A)*), pTB99 (*pdpy-7::egl-15(5A)ecto*), and pTB114 (*pF25B3.3::egl-15(5A)*) were kindly provided by Dr. H. Bülow. NH112 (*EGL-15*) were kindly provided by T. Kinnunen. *Pdpy-4::gfp::cup-5* was built modified from pHD423, which was kindly provided by Dr. H. Fares. *Pdpy-4::tom20::yfp*, *Pdpy-4::gfp::rab-7*, *Pdpy-4::gfp::rab-5* were modified from *Pmig-13::tom20::yfp*, *Pmig-13::gfp::rab-7*, *Pmig-13::gfp::rab-5* from Dr. K. Shen. The remaining constructs were listed in Table S2.

**SUPPLEMENTAL REFERENCES**

Lo, T.W., Branda, C.S., Huang, P., Sasson, I.E., Goodman, S.J., and Stern, M.J. (2008). Different isoforms of the *C. elegans* FGF receptor are required for attraction and repulsion of the migrating sex myoblasts. *Dev. Biol.* 318, 268–275.

Saitou, N., and Nei, M. (1987). The neighbor-joining method: a new method for reconstructing phylogenetic trees. *Mol. Biol. Evol.* 4, 406–425.

Tamura, K., Peterson, D., Peterson, N., Stecher, G., Nei, M., and Kumar, S. (2011). MEGA5: molecular evolutionary genetics analysis using maximum likelihood, evolutionary distance, and maximum parsimony methods. *Mol. Biol. Evol.* 28, 2731–2739.

Zuckerklund, E., and Pauling, L. (1965). Evolutionary divergence and convergence in proteins. In *Evolving Genes and Proteins*, V.B.a.H.J. Vogel, ed. (New York: Academic Press), pp. 97–166.

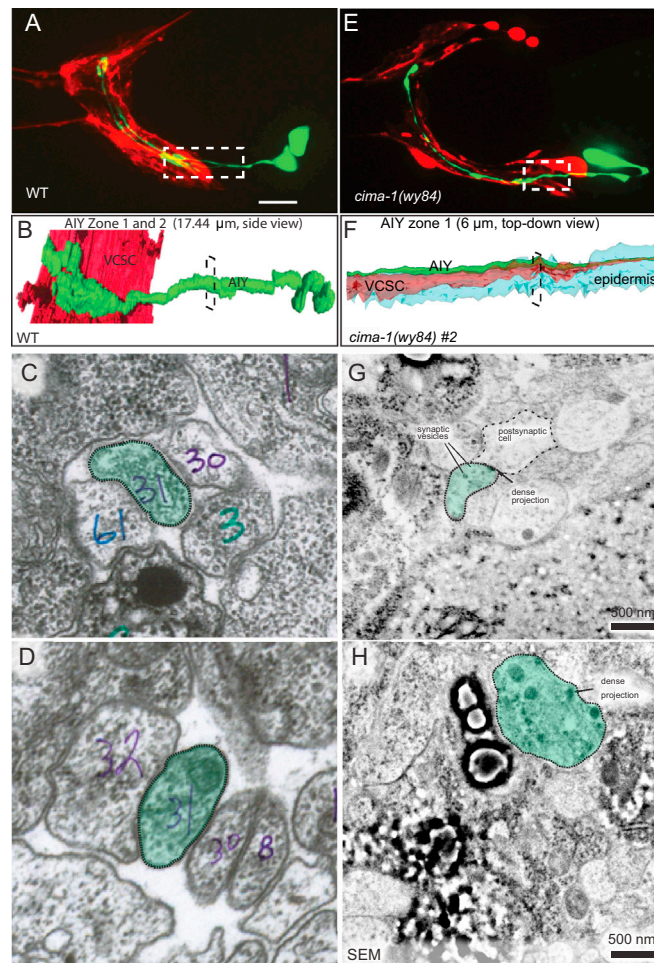


**Figure S1. fEM Reconstruction of AIY, VCSC Glia, and Epidermal Cell *hyp7* in *cima-1(wy84)* Mutants, Related to Figures 1 and 6**

(A) AIY (green) and VCSC glia (red) are simultaneously visualized in wild-type animals

Dashed box corresponds to the region reconstructed in (B).

(B) Reconstruction of the left AIY (green) and the VCSC glia (red) using micrographs for wild-type animals available from WormImage ([www.wormimage.org](http://www.wormimage.org)). The micrographs used for the reconstruction were originally photographed to describe *C. elegans* nervous system connectivity in (White et al., 1986) and were made available to us by Dr. David Hall (Albert Einstein College of Medicine). We reconstructed the zone 1 and zone 2 regions for both the N2U and JSH data sets. The reconstruction shown here corresponds to the N2U data set, but similar results were observed for the JSH data set (data not shown). Note that in wild-type animals, the VCSC glia ensheath the zone 2 region, but not the zone 1 region, consistent with what we saw with our fluorescent and GRASP markers.

(C and D) Representative cross-section EM micrographs for the zone 1 region in wild-type animals. In (C), the image corresponds to the JSH data set, which was obtained from a wild-type L4 animal. In (D), the image corresponds to the wild-type adult N2U data set. In both images, AIY is pseudocolored green and highlighted with a dashed line. Note the absence of dense projections or synaptic vesicles in this region of the AIY neurite (compare to Figure 5A, where dense projections and synaptic vesicles are seen in the AIY neurite). We inspected all wild-type zone 1 EM micrographs for JSH and N2U animals, and did not detect dense projections or vesicles in any of them, consistent with what we observed for our synaptic markers in AIY. The electron micrograph is of animals "JSH" and "N2U shown with permission," each was prepared by J. White, E. Southgate, N. Thomson, and S. Brenner at the LMB/MRC labs in Cambridge, England (White et al., 1986). With help from John White, the JSH and N2U image archives are now conserved in the Hall lab in NYC, and available online at <http://www.wormimage.org>.

(E) As in (A), but *cima-1(wy84)* mutant adult animal. Dashed box corresponds to the region reconstructed in (F).

(F) Reconstruction of AIY (green), VCSC glia (red) and epidermal cell (blue) from a *cima-1(wy84)* mutant adult animal by using fluorescent EM (fEM). The AIY neurite was identified by the cell-specific expression of GFP. VCSC glia and epidermis were identified by cell position.

(G and H) Representative cross-section EM micrographs for the zone 1 region in two *cima-1(wy84)* mutant animals visualized by fEM. AIY is pseudocolored in green and highlighted with a dashed line. Unlike wild-type animals, in *cima-1(wy84)* adult animals we observed dense projections and synaptic vesicles in the zone 1 region. In (G) we highlight a neighboring neuron onto which the ectopic AIY dense projection could be forming.

Scale bars in G and H also apply to C and D.

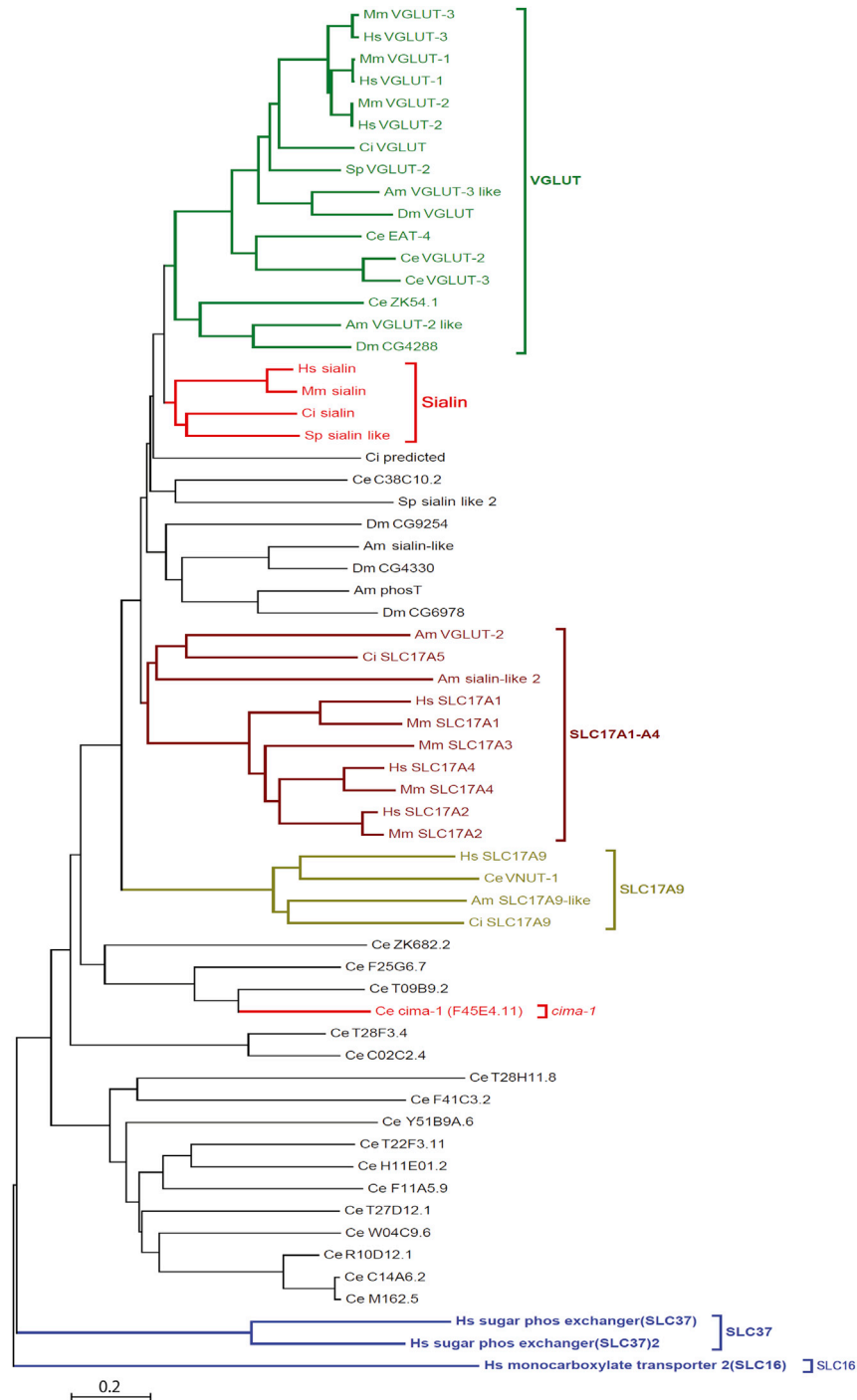


**Figure S2. CIMA-1 Is a Member of SLC17 Family, Related to Figure 3**

A diagram of phylogenetic relationship among solute carrier transporters. Phylogenetic topology was based on the cluster W alignment of SLC17 family proteins from human (Hs: *Homo sapiens*), mouse (Mm: *Mus musculus*), honeybee (Ap: *Apis mellifera*), fruit fly (Dm: *Drosophila melanogaster*), sea urchin (Sp: *Strongylocentrotus purpuratus*), sea squirt (Ci: *Ciona intestinalis*), nematode (Ce: *Caenorhabditis elegans*). Two human SLC37 family proteins and one SLC16 family protein were selected to root the tree. The tree is constructed by using the NJ (neighbor-joining) method (Saitou and Nei, 1987). The tree is made with NJ (neighbor-joining) method (Saitou and Nei, 1987). The branch lengths correspond to evolutionary distances and were computed using the Poisson correction method (Zuckerkind and Pauling, 1965). The unit is the number of amino acid substitutions per site. Evolutionary analyses were conducted in MEGA5 (Tamura et al., 2011). As shown in the tree, *cima-1* forms a cluster with SLC17, but not with SLC16 or SLC37. SLC: solute carrier, PhosT: Phosphate transporter, Hs SLC37: sugar phosphate exchanger, Hs SLC16: monocarboxylate transporter 2.

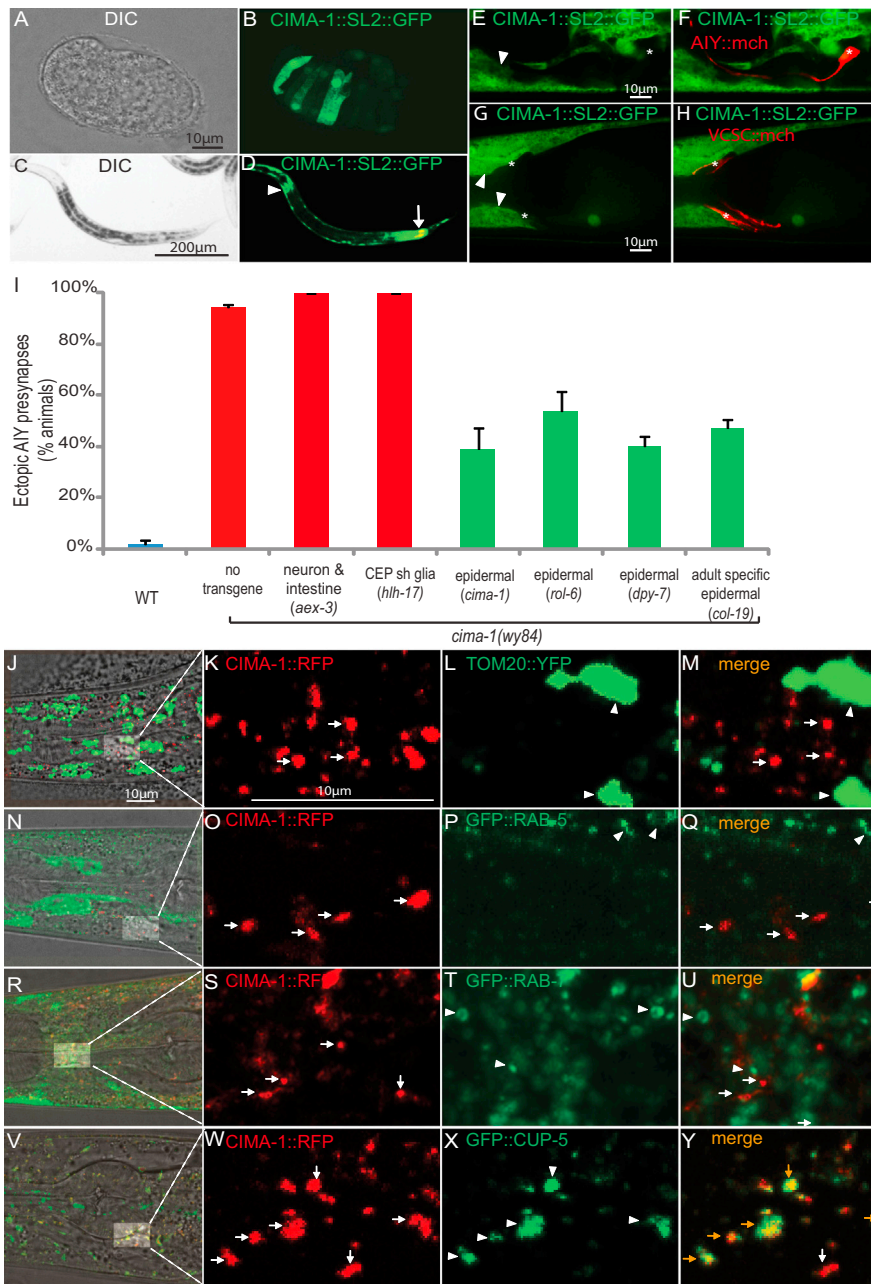


**Figure S3. *cima-1* Is Expressed and Required in Epidermal Cells, Related to Figure 4**

(A-H), CIMA-1(genomic)::SL2::GFP is expressed in the embryo (A, B), larval (C, D), and adult stages (E-H) in the intestine (D, as indicated by the arrow) and in epidermal cells (D, E and G, as indicated by arrow heads), but not in the AIY interneuron (E, F) or VCSC glia (G, H) (as indicated by asterisk). The AIY interneuron and the VCSC glia were colabeled with cytoplasmic mCherry (F, H).

(I) Cell-specific expression of *cima-1* cDNA in neurons/intestine (*aex-3* promoter) and in VCSC glia (*hlh-17* promoter) does not result in rescue. However, endogenous expression (*cima-1* promoter) or tissue-specific expression in epidermal cells (*rol-6*, *dpy-7* and *col-19* promoter) rescues the AIY presynaptic defect. *Pcol-19* promoter drives expression after larval stages and in epidermal cells (Cox and Hirsh, 1985; Liu and Ambros, 1991). Therefore rescue using the *Pcol-19* suggests that *cima-1* acts postdevelopmentally in epidermal cells. Error bars are SEM.

(J-Y) CIMA-1 protein fused to RFP (CIMA-1::RFP) is coexpressed in epidermal cells with mitochondrial marker TOM20::YFP (J-M), early endosomal marker GFP::RAB-5 (N-Q), later endosome GFP::RAB-7 (R-U), and lysosomal marker GFP::CUP-5 (V-Y). White arrows indicate CIMA-1::RFP, arrow heads indicate GFP-marked proteins and orange arrows indicate the colocalization of CIMA-1::RFP and GFP-marked proteins. Notice that CIMA-1::RFP is largely colocalized with lysosomal marker GFP::CUP-5. Consistent with this, Pearson's correlation coefficient for CIMA-1 and CUP-5 is 0.53 (for the other markers: CIMA-1 and TOM20 is 0.021; CIMA-1 and RAB-5 is 0.22; CIMA-1 and RAB-7 is 0.28). The scale bar in J applies to N, R, and V; scale bar in K applies to L-M, O-Q, S-U and W-Y.

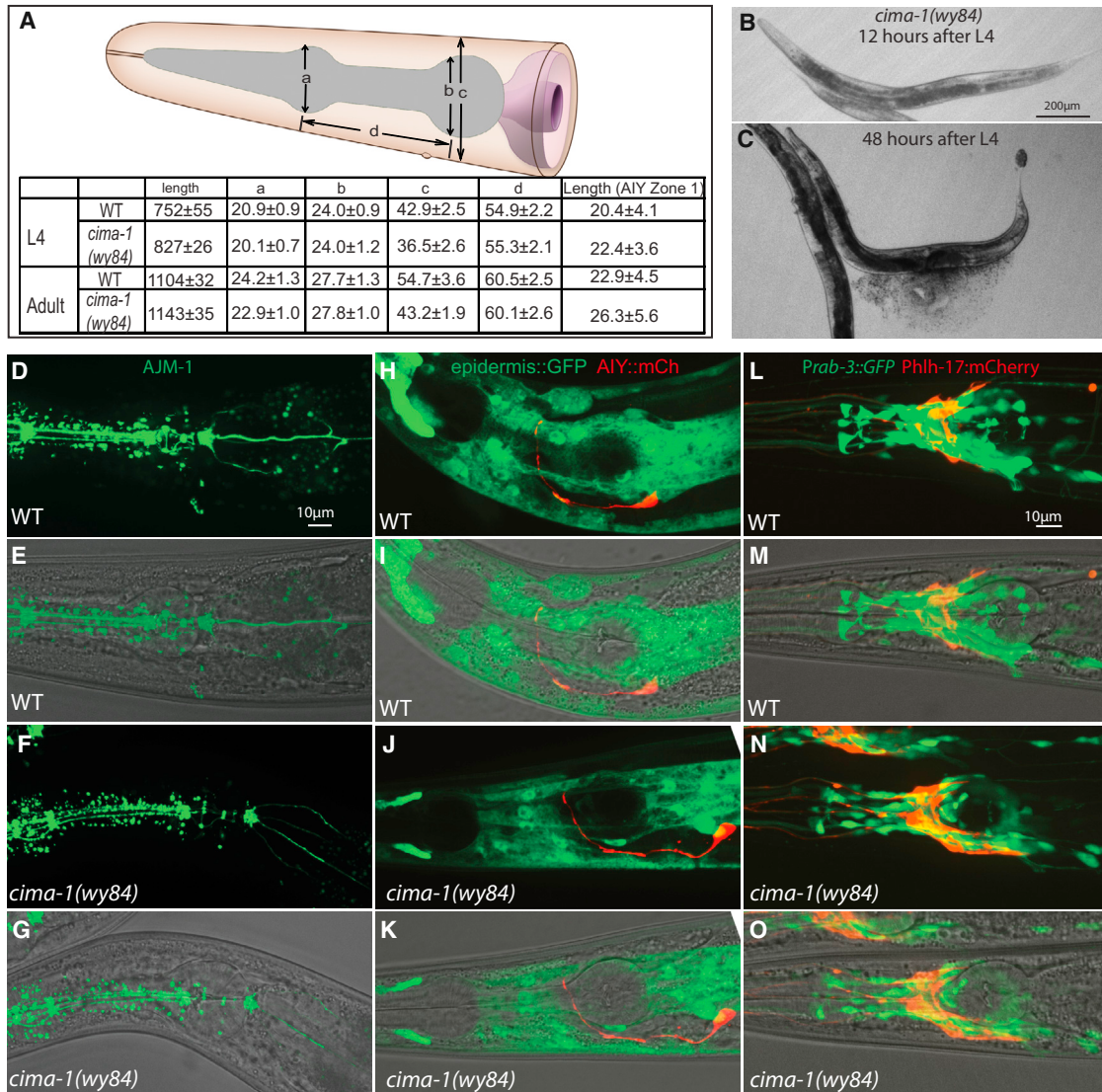


**Figure S4. Morphological Phenotypes in *cima-1(wy84)* Adult Animals, Related to Figure 4**

(A) Quantification of length, width, pharyngeal morphology and length of AIY zone 1 (as indicated in Figure 1A) for wild-type and *cima-1(wy84)* animals (L4 and adults, as stated in the table). Parameters are indicated in the schematic. Note that *cima-1(wy84)* mutant animals are slightly longer for both body and AIY zone 1 length, although the pharyngeal morphology is similar to wild-type animals. The numbers are mean  $\pm$  SD.

(B and C) *cima-1(wy84)* animals 12 hr after L4 (B) and *cima-1(wy84)* animals two days after L4. (C) Some 2- to 3-day-old *cima-1(wy84)* mutants burst at the vulva. All of the analyses presented here regarding glia positions and presynaptic pattern in AIY were done in *cima-1(wy84)* adult animals before this period.

(D–G) Wild-type (D and E) and *cima-1(wy84)* (F and G) adult animals labeled with epidermal cell junction marker AJM-1::GFP. No differences were noticed in the localization of AJM-1::GFP or regarding cellular fusions during development.

(H–K) Wild-type (H and I) and *cima-1(wy84)* (J and K) adult animals labeled with epidermal GFP (*cima-1* promoter) and AIY mCherry (*ttx-3* promoter) were imaged and characterized ( $n > 10$  animals). No abnormalities were noticed regarding epidermal cells morphology between *cima-1(wy84)* and wild-type animals.

(L–O) *prab-3::GFP* and *phlh-17::mCherry* in wild-type (L and M) and *cima-1(wy84)* mutant (N and O). No abnormalities were noticed regarding neuronal distribution between *cima-1(wy84)* and wild-type animals, but notice how glia are posteriorly distended in *cima-1(wy84)* mutant adults.

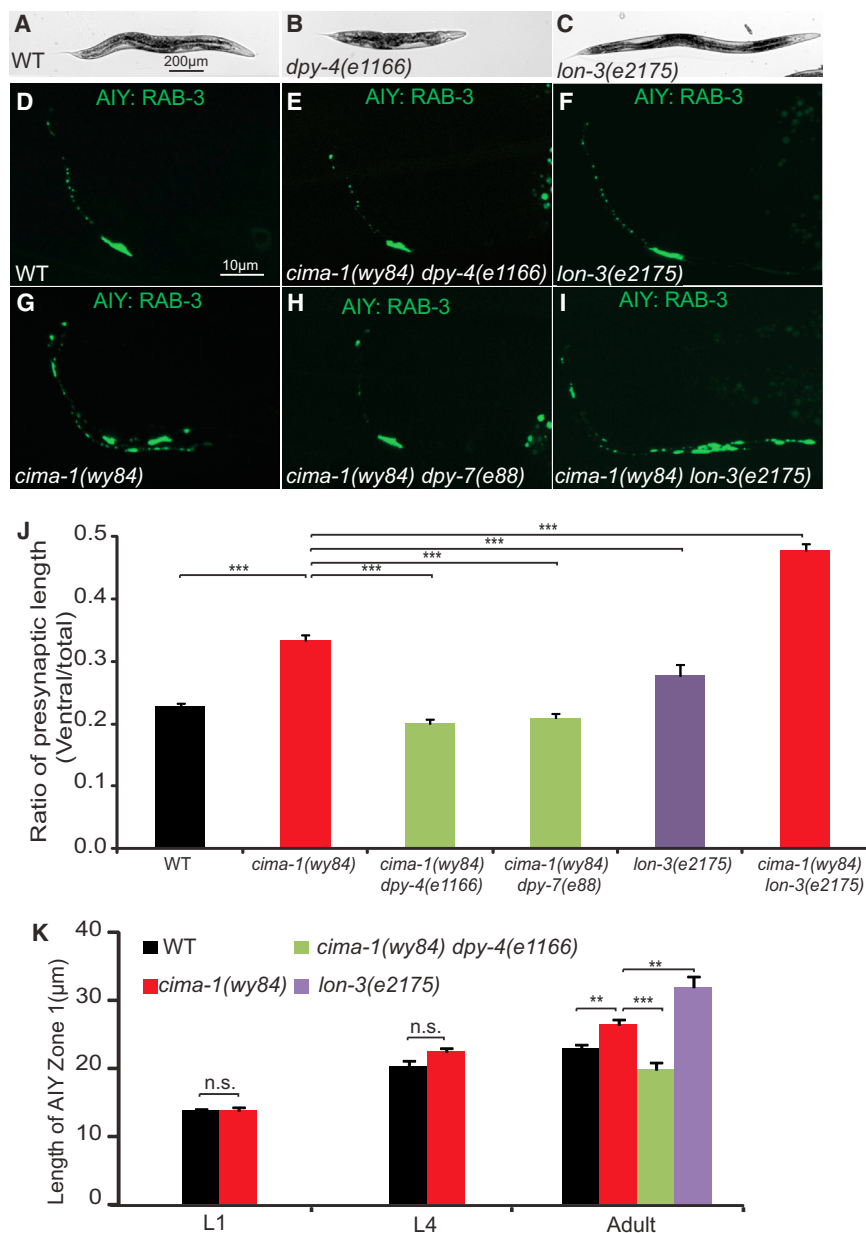


**Figure S5. Expressivity of the AIY Presynaptic Defect in *cima-1(wy84)* Is Affected by Size of the Animal, Related to Figure 4**

(A–C) Morphology of wild-type, *dpy-4(e1166)*, and *lon-3(e2175)* animals.

(D–I) AIY presynaptic marker GFP::RAB-3 in wild-type (D), *cima-1(wy84)* (G), *cima-1(wy84) dpy-4(e1166)* (E), *cima-1(wy84) dpy-7(e88)* (H), *lon-3(e2175)* (F) and *cima-1(wy84) lon-3(e2175)* (I) animals. Note that *dpy* mutants suppress *cima-1(wy84)* AIY presynaptic defect, and *lon-3(e2175)* enhances *cima-1(wy84)* phenotype.

(J and K) Quantification of AIY presynaptic pattern (J) and zone 1 length (K). In (J), the ratio of the presynaptic length (see Figure 1K) is a metric that reflects the presynaptic pattern of AIY. Note how AIY presynaptic ratio defect in *cima-1(wy84)* animals is suppressed by *dpy-4(e1166)* and *dpy-7(e88)* and enhanced by *lon-3(e2175)*. In (K), for wild-type and *cima-1(wy84)* animals, the length of AIY zone 1 was measured at larval L1, L4 and adult stages. For *lon-3(e2175)* and *cima-1(wy84) dpy-4(e1166)* animals, it was measured only at adult stage. Note that at L1 or L4 stage, the length of AIY zone 1 is not significantly different between wild-type and *cima-1(wy84)* mutant animals. At adult stage, however, it is significantly longer in *cima-1(wy84)* animals. Although AIY zone 1 is longer in *lon-3(e2175)* mutants (see K), *lon-3(e2175)* animals do not phenocopy *cima-1(wy84)* mutants. Therefore, it is not the increase in the length of the AIY axon that causes ectopic synapses in *cima-1(wy84)* mutants, rather it is a specific requirement for *cima-1*. Error bars are SEM. \*\**p* < 0.01, \*\*\**p* < 0.001 by *t* test comparison.

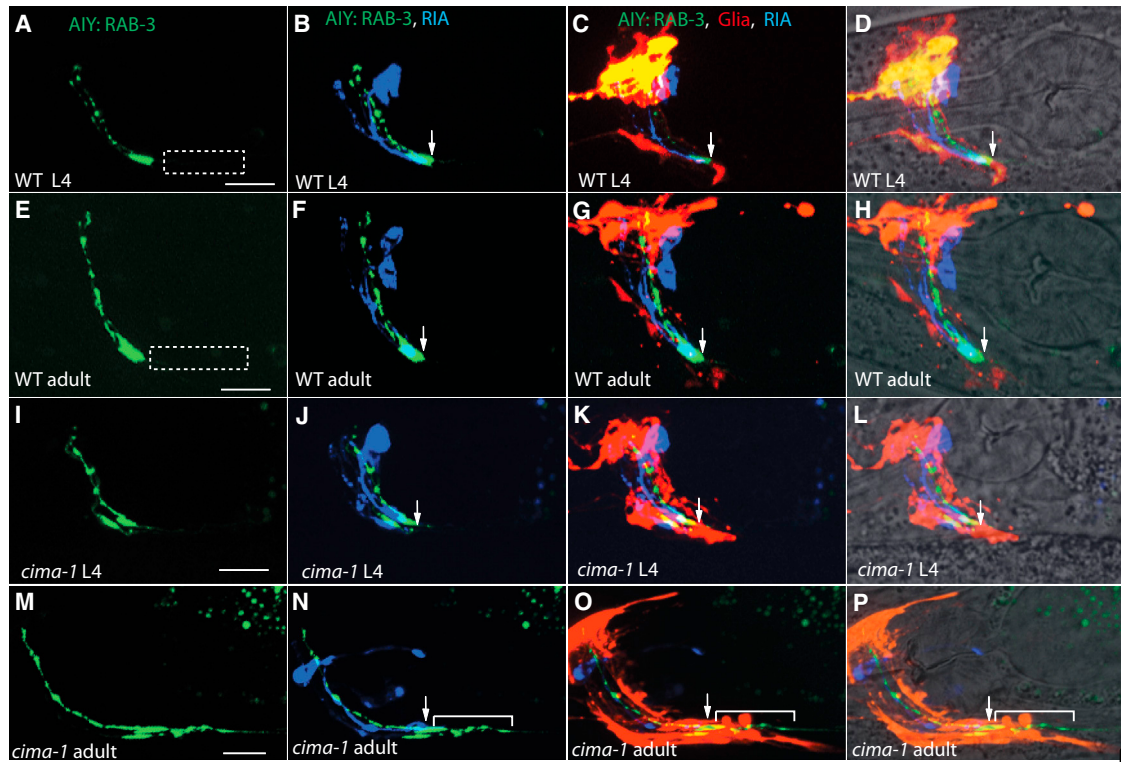


**Figure S6. Longitudinal Analyses of Glial Morphology, RIA Position and AIY Presynaptic Pattern in Wild-Type and *cima-1(wy84)* Animals, Related to Figure 5**

(A–H) A single wild-type animal labeled with AIY presynaptic CFP::RAB-3 (pseudocolored green), RIA postsynaptic GLR-1::YFP (pseudocolored blue) and VCSC glia cytoplasmic mCherry was imaged at juvenile L4 stage (A–D), and 48 hr later at adult stage (E–H).

(I–P) A single *cima-1(wy84)* animal was imaged at juvenile L4 (I–L) and 48 hr later at adult stage (M–P). Arrows highlight the end of zone 2 and beginning of zone 1, and brackets corresponds to ectopic presynaptic sites in zone 1 region.

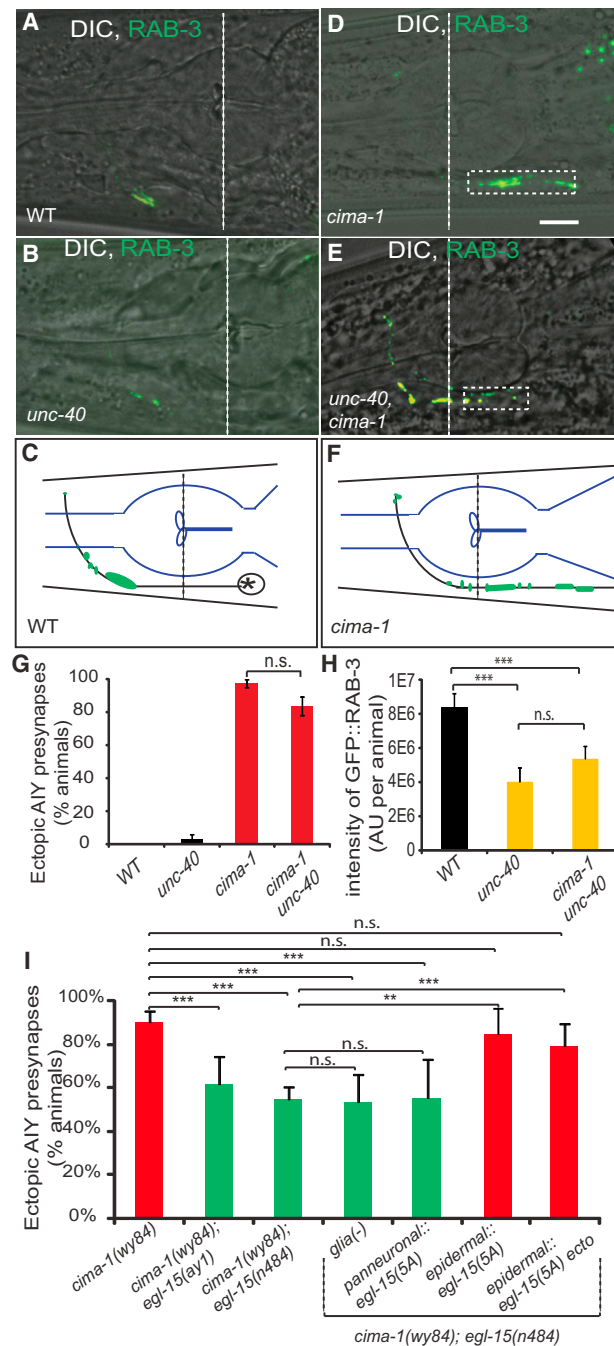


**Figure S7. *egl-15(n484)*, but Not *unc-40(e271)*, Suppress *cima-1*, Related to Figure 7**

(A–C) Presynaptic marker GFP::RAB-3 in wild-type (A) or *unc-40(e271)* mutants (B). Schematic drawing of a wild-type animal in (C).

(D–F) As in (A–C), but in *cima-1(wy84)* adult animals (D) or *cima-1(wy84) unc-40(e271)* double mutants adult animals (E).

(G) Quantification of the percentage of animals displaying ectopic presynaptic sites in the zone 1 region of AIY. Note how *unc-40(e271)* does not suppress the number of animals displaying ectopic presynaptic sites in zone 1 in *cima-1(wy84)*. Error bars represent 95% confidential interval. n.s.: not significant based on Fisher's exact test.

(H) Quantification of intensity of AIY synaptic vesicle marker GFP::RAB-3 in larval stage 1 (L1) animals for indicated genotypes. AU: arbitrary unit. Error bars represent SEM. n.s.: not significant, \*\*\*:  $p < 0.001$  with t-student test.

(I) Quantification of the percentage of animals displaying ectopic presynaptic sites in zone 1 for examined genotypes. Error bars represent 95% confidential interval. n.s.: not significant, \*\* $p < 0.01$ , \*\*\* $p < 0.001$  between groups by using Fisher's exact test.